











# STOP1 activates NRT1.1-mediated nitrate uptake to create a favorable rhizospheric pH for plant adaptation to acidity

Jia Yuan Ye <sup>1</sup>, Wen Hao Tian <sup>2</sup>, Miao Zhou <sup>1</sup>, Qing Yang Zhu <sup>1</sup>, Wen Xin Du <sup>1</sup>,  
Ya Xin Zhu <sup>1</sup>, Xing Xing Liu <sup>1</sup>, Xian Yong Lin <sup>1</sup>, Shao Jian Zheng <sup>2</sup> and Chong Wei Jin <sup>1,†,\*</sup>

1 State Key Laboratory of Plant Physiology and Biochemistry, College of Natural Resources and Environmental Science, Zhejiang University, Hangzhou 310058, China

2 State Key Laboratory of Plant Physiology and Biochemistry, College of Life Science, Zhejiang University, Hangzhou 310058, China

\*Author for correspondence: jincw@zju.edu.cn

†Senior author.

C.W.J. conceived the project. J.Y.Y. and C.W.J. designed the experiments. J.Y.Y. and W.H.T. performed the majority of experiments. M.Z., Q.Y.Z., W.X.D., Y.X.Z., and X.X.L. assisted in performing the experiments and analyzing the data. J.Y.Y. and C.W.J. interpreted the data, generated the figures, and wrote the manuscript. X.Y.L. and S.J.Z. provided suggestions and revised the manuscript.

The author(s) responsible for distribution of materials integral to the findings presented in this article in accordance with the policy described in the Instructions for Authors (<https://academic.oup.com/plcell>) is: Chong Wei Jin (jincw@zju.edu.cn)

## Abstract

Protons ( $H^+$ ) in acidic soils arrest plant growth. However, the mechanisms by which plants optimize their biological processes to diminish the unfavorable effects of  $H^+$  stress remain largely unclear. Here, we showed that in the roots of *Arabidopsis thaliana*, the C2H2-type transcription factor STOP1 in the nucleus was enriched by low pH in a nitrate-independent manner, with the spatial expression pattern of *NITRATE TRANSPORTER 1.1* (*NRT1.1*) established by low pH required the action of STOP1. Additionally, the *nrt1.1* and *stop1* mutants, as well as the *nrt1.1 stop1* double mutant, had a similar hypersensitive phenotype to low pH, indicating that STOP1 and NRT1.1 function in the same pathway for  $H^+$  tolerance. Molecular assays revealed that STOP1 directly bound to the promoter of *NRT1.1* to activate its transcription in response to low pH, thus upregulating its nitrate uptake. This action improved the nitrogen use efficiency (NUE) of plants and created a favorable rhizospheric pH for root growth by enhancing  $H^+$  depletion in the rhizosphere. Consequently, the constitutive expression of *NRT1.1* in *stop1* mutants abolished the hypersensitive phenotype to low pH. These results demonstrate that STOP1-NRT1.1 is a key module for plants to optimize NUE and ensure better plant growth in acidic media.

## Introduction

Acidic soils are widespread, covering 40%–50% of the world's total arable lands (Kochian et al., 2015). Unfortunately, current human activities, particularly the use of nitrogen (N) fertilizers, including urea and ammonium, continuously aggravate soil acidification (Guo et al., 2010; Kissel et al.,

2020). High proton ( $H^+$ ) concentrations are toxic and repress nutrient acquisition in plants (Schubert and Mengel, 1990; Iuchi et al., 2007), which aggravates nutrient loss and increases the risk of environmental pollution. The  $H^+$  in acidic soils also induces many other stress factors, such as aluminum ( $Al^{3+}$ ) toxicity and phosphate (Pi) deficiency (Sawaki et al., 2009; Kochian et al., 2015). As a result, soil acidity is a

## IN A NUTSHELL

**Background:** Acid soils cover nearly half of the world's arable lands. Application of urea-N and ammonium-N fertilizers markedly increases soil acidification due to proton ( $H^+$ ) generation from nitrification. High  $H^+$  concentrations in acid soils are highly rhizotoxic to most plants, thereby arresting their growth and productivity. Genetic manipulation of plants to optimize their biological processes and improve their adaptation to acid soils may be a cost-effective means of improving plant production in these soils. However, our current knowledge of  $H^+$  tolerance mechanisms is quite limited.

**Question:** Can we optimize plant biological processes to diminish the unfavorable impacts of  $H^+$  stress via the action of *STOP1*, the first key gene for  $H^+$  tolerance identified in plants that encodes a C2H2-type transcription factor?

**Findings:** We showed that in *Arabidopsis* roots, low pH enrichment of nuclear *STOP1* directly activates *NITRATE TRANSPORTER 1.1 (NRT1.1)* expression by binding to its promoter and stimulating  $H^+$ -coupled  $NO_3^-$  uptake by *NRT1.1*. This action enhances  $H^+$  depletion in the rhizosphere, creating a favorable rhizospheric pH for root growth and increasing N recovery from acid soils by plants. Therefore, *STOP1-NRT1.1* is a key module by which plants improve nitrogen use efficiency, ensuring better plant growth under acidic conditions.

**Next steps:** We plan to elucidate how roots avoid an excess accumulation of  $H^+$  in the cytoplasm after stimulating  $H^+$ -coupled  $NO_3^-$  uptake by *NRT1.1*. We also aim to clarify the basis of signaling leading to enrichment of nucleus-localized *STOP1* in response to  $H^+$  stress.

main constraint in crop production (Kochian et al., 2015). Molecular breeding of plants to improve nutrient acquisition and adaptation to acidic soils may be a cost-effective solution to these problems (Schroeder et al., 2013). However, our current understanding of the mechanisms underlying  $H^+$  tolerance and its coordination of nutrient acquisition is limited.

The identification of an *Arabidopsis thaliana* mutant hypersensitive to  $H^+$  rhizotoxicity (*stop1*) enabled the identification of the first key  $H^+$ -tolerance gene, encoding the C2H2-type zinc finger transcription factor SENSITIVE TO PROTON RHIZOTOXICITY1 (*STOP1*; Iuchi et al., 2007). This transcription factor was later determined to regulate the growth responses to many environmental cues, including  $Al^{3+}$  toxicity, Pi deficiency, salt stress, drought, and low-oxygen stress (Sawaki et al., 2009; Balzergue et al., 2017; Mora-Macías et al., 2017; Enomoto et al., 2019; Godon et al., 2019; Sadhukhan et al., 2019). Despite the fact that *STOP1* was found to act in  $H^+$  tolerance over a decade ago, the target genes and underlying biological mechanisms via which *STOP1* regulates  $H^+$  tolerance remain unclear.

Although high concentrations of  $H^+$  in acidic rooting media are highly toxic, a modest dose of  $H^+$  is essential for plants. In fact,  $H^+$  gradients established across cellular membranes drive the nutrients uptake by the root cells (Shavrukov and Hirai, 2015). By contrast, the uptake of some nutrients such as nitrate ( $NO_3^-$ ) and potassium ( $K^+$ ) by root cells also leads to the influx or efflux of  $H^+$  (Haynes, 1990; Feng et al., 2020). In the context of this interplay, there may be a relationship between  $H^+$  tolerance and nutrient acquisition by roots. As mentioned above, the application of urea-N and ammonium-N fertilizers markedly accelerates

soil acidification because of  $H^+$  generation from nitrification (Guo et al., 2010; Kissel et al., 2020). If the  $H^+$  influx due to nutrient acquisition by plants could balance or partially balance the  $H^+$  generated by N fertilizers, the acidification of the soil may be slowed down, which is favorable for both the agricultural ecosystem and plant production.

In this study, we identified a biological pathway that was beneficial for both ecosystems and plants under acidic conditions: in *Arabidopsis*, low pH-enhanced *STOP1* directly bound to the promoter of *NITRATE TRANSPORTER 1.1 (NRT1.1)* to facilitate its expression, thereby enhancing the  $H^+$ -coupled uptake of  $NO_3^-$  by roots to improve the N use efficiency (NUE) of plants; this process also enhanced  $H^+$  depletion in the rhizosphere, avoiding  $H^+$  toxicity in plants by creating a favorable rhizospheric pH. Our findings may provide a strategy for improving the NUE of plants to partially counter the  $H^+$  generated from N fertilizers and ensuring better plant production in acidic soils through the manipulation of the *STOP1-NRT1.1* module.

## Results

### *STOP1* is required for better plant growth and N recovery from acidic soil

Although *STOP1* has been demonstrated to be required for both the  $H^+$  and  $Al^{3+}$  tolerance of *Arabidopsis* in agar medium (Iuchi et al., 2007), its performance in acidic soil conditions needs to be verified further. Given that *Arabidopsis* is slightly sensitive to either  $H^+$  or  $Al^{3+}$  stress (Kobayashi et al., 2013; Ito et al., 2019), a moderately acidified soil (A1-soil) with an initial pH of 5.44 was used for verification in this study. In addition, plant growth in neutral soil (N-soil) with

an initial pH of 7.04 was used as control. Urea was used as the N fertilizer because it is the most commonly used in current agricultural practices. The plants were harvested after a 5-week period of growth. The pH of the soils at harvest was determined using a glass electrode (1:2.5 soil:water ratio). A1-soil and N-soil pH decreased to 4.74–5.15 and 6.66–6.83, respectively, showing that the nitrification of urea resulted in acidification of these soils. As expected, the Col-0 and STOP1-null mutants (*stop1<sup>KO</sup>* and *stop1-3*) had similar growth in N-Soil (Supplemental Figure S1, A and B); the STOP1-null mutants had clear growth retardation in the A1-soil (Figure 1A), with both shoot biomass decreasing by ~40% compared with Col-0 plants (Supplemental Figure S1C). Since high levels of H<sup>+</sup> and Al<sup>3+</sup> co-exist in acidic soils, we attempted to distinguish the effects of these two stress factors on the growth of *stop1* mutants. STOP1 regulates Al<sup>3+</sup> tolerance by directly activating its target gene, *ALMT1* (Sawaki et al., 2009). However, the *almt1* knockout mutants displayed a similar growth phenotype to Col-0 plants in A1-soil (Figure 1A), indicating that the growth retardation of *stop1* mutants in this acidic soil was not due to Al<sup>3+</sup> toxicity, but was more likely associated with H<sup>+</sup> toxicity.

Given that N is quantitatively the most important nutrient for plant growth and productivity, we also analyzed the N content of the plants grown in A1-soil. Our results showed that the loss of function of STOP1 significantly reduced the N content in the shoots of the *stop1* mutants (Figure 1B). To evaluate the N recovery efficiency from the N resources in A1-soil, we calculated the N uptake efficiency (NUpE) and NUE, which are defined as the proportion of N acquired by plants from the N fertilizer and the plant biomass produced per unit of N fertilizer, respectively (Xu et al., 2012). Because the roots of Arabidopsis are critically thin and difficult to harvest intact from soils, only the N content and biomass of shoot parts were used for NUpE and NUE calculations. The values of both indices were lower in *stop1* mutants than in Col-0 plants (Figure 1, C and D), suggesting that STOP1 is required to ensure better N recovery from acidic soils by plants.

### STOP1-conferred H<sup>+</sup> tolerance depends on an increase in rhizospheric pH

Notably, when Col-0 and *stop1<sup>KO</sup>* were co-planted in A1-soil fertilized with urea, the growth of *stop1<sup>KO</sup>* was improved to a level similar to that of Col-0 (Figure 2A; Supplemental

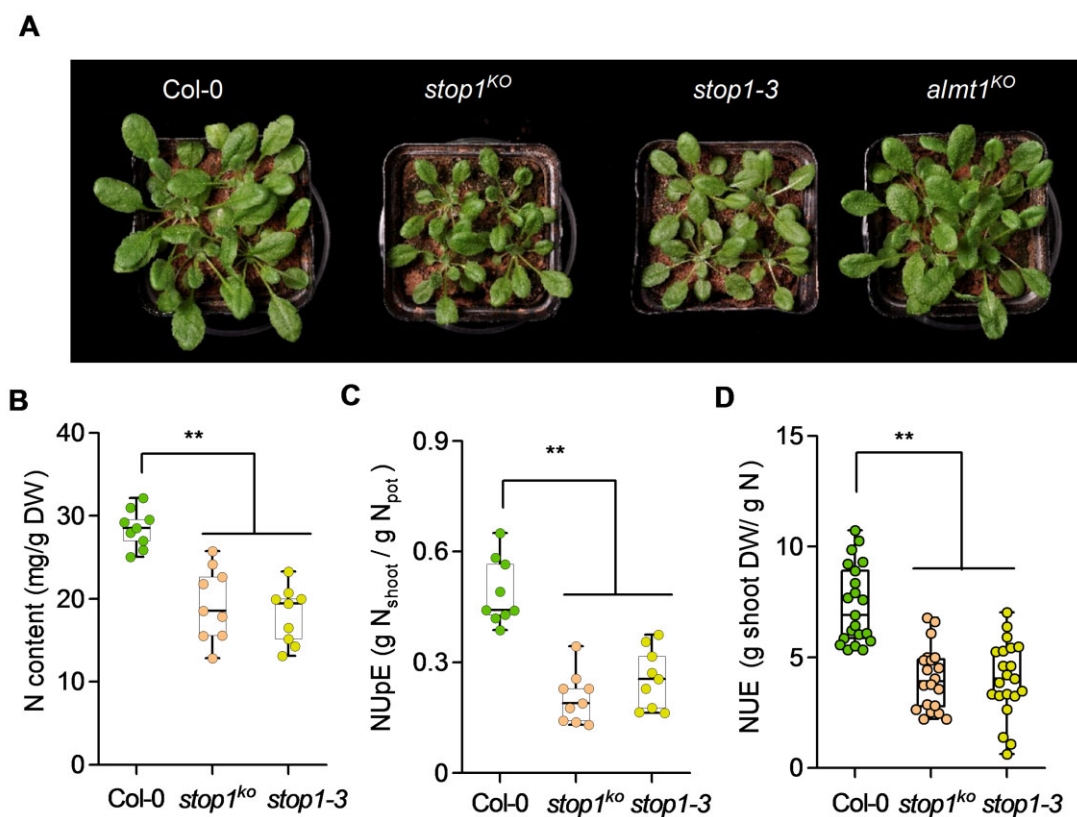


**Figure 1** STOP1 promotes plant growth and N recovery from acidic soil. A, Growth phenotypes of Col-0, *stop1*, and *almt1<sup>KO</sup>* plants. B, N content in shoots. C, N uptake efficiency (NUpE). D, NUE. The whiskers indicate the minimum and maximum values; the boxes show the means  $\pm$  sd of 9 seedlings in (B and C) and of 21 seedlings in (D). The plants were grown in pots with moderately acidified soil (initial pH = 5.44). The pots were weighed and watered daily to maintain a relatively constant humidity. The plants in each pot were fertilized weekly with 0.005 g of urea and harvested for analysis after a 5-week period of growth. NUpE was calculated as shoot N/N in pots, and NUE was calculated as dry shoot biomass/N in pots. All experiments were repeated independently twice, with similar results, and one representative experiment is shown. Asterisks show significant differences compared with Col-0 using one-way ANOVA followed by Tukey's multiple comparison test (\* $P < 0.05$ , \*\* $P < 0.001$ ).



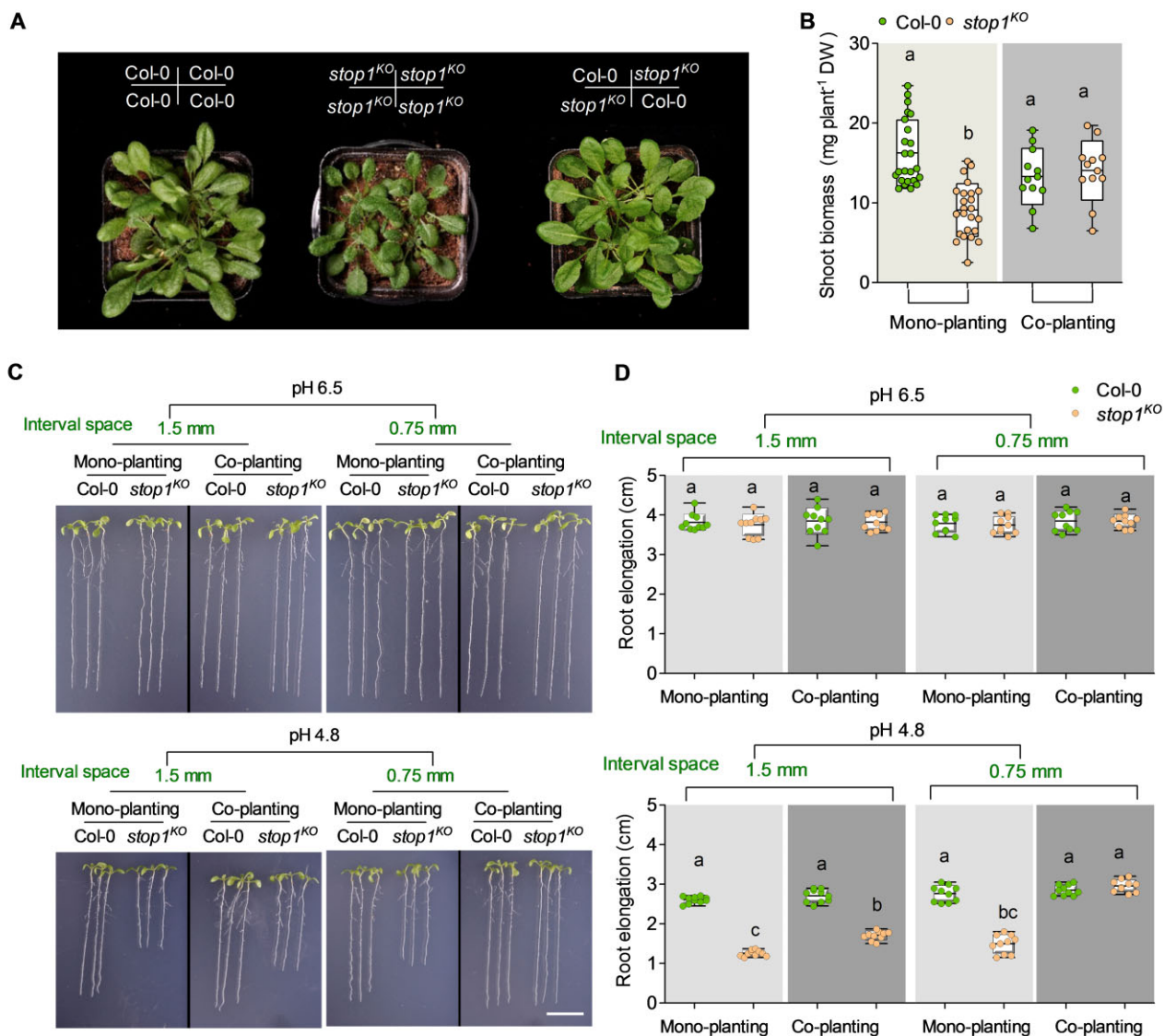


**Figure 2** Col-0 and *stop1<sup>KO</sup>* co-planting improves the growth of *stop1<sup>KO</sup>* in acidic conditions. A and B, Growth of mono-planted and co-planted plants in acidic soil. The treatments are the same as those in Figure 1. The whiskers indicate the minimum and maximum values; the boxes are presented as the mean  $\pm$  SD of 12 or 24 seedlings. C and D, Root growth of mono-planted and co-planted seedlings in acidic agar medium. The whiskers indicate the minimum and maximum values; the boxes are presented as the mean  $\pm$  SD of 10 seedlings. The 3-day-old Col-0 and *stop1<sup>KO</sup>* seedlings were mono-planted or co-planted at different interval spaces in neutral or low pH agar medium, as depicted in Supplemental Figure S3. Seedlings were transferred to be registered as pictures and root elongation was analyzed 3 days after treatment. Scale bar: 1 cm. Each experiment was repeated independently three times with similar results, and a representative experiment is shown. Different letters indicate significant differences between means ( $P < 0.05$ ; two-way ANOVA in (B) and multiway ANOVA in (D) with Tukey's multiple comparisons test.

Figure S2). We also examined the effect of co-planting them on the growth of *stop1<sup>KO</sup>* in nitrate-fertilized soil. Considering the absence of nitrification-caused acidification, a soil (A2-soil; initial pH = 5.07) more acidic than A1-soil was used in this experiment. Similarly, co-planting with Col-0 also helped the growth of *stop1<sup>KO</sup>* in A2-soil when fertilized with nitrate (Supplemental Figure S2). These results suggest that STOP1-conferred H<sup>+</sup> tolerance is associated with the rhizosphere process. The effect of Col-0 and *stop1<sup>KO</sup>* co-planting on root growth of *stop1<sup>KO</sup>* was also tested in agar media (Figure 2; Supplemental Figure S3). In

our current study, 6-mM NO<sub>3</sub><sup>-</sup> and 2-mM NH<sub>4</sub><sup>+</sup> were used as the N sources for agar media. In comparison with mono-planting treatment, Col-0 and *stop1<sup>KO</sup>* co-planting with an interval space at 1.5 mm had little effect on their root growth in natural-pH conditions, but improved the root growth of *stop1<sup>KO</sup>* in low-pH conditions. When the interval space between the two co-planted plants was decreased to 0.75 mm, the root growth of *stop1<sup>KO</sup>* improved to a level similar to that of Col-0 in low-pH conditions. This result provides a further support to our conclusion that STOP1-conferred H<sup>+</sup> tolerance depends on the rhizospheric process.

A simple rhizospheric process expected to improve root growth in an acidic medium may be an increase in rhizospheric pH. To test this hypothesis, seedlings were grown in an acidic agar medium with or without pH buffer Homo-PIPES, which was used to minimize pH alteration. The 0.75 mM of Homo-PIPES was selected to treat the acidic medium because this dose did not affect the root growth of seedlings in a neutral-pH medium (Supplemental Figure S4). As shown in Figure 3, A and B, the root growth of either Col-0 or the complementation line (COM), generated by expressing *pSTOP1:GFP-STOP1* in *stop1*<sup>KO</sup> (Balzergue et al., 2017), was greatly inhibited in the low-pH agar medium with pH buffering, and consequently did not differ from that of the *stop1* mutants. This was contrary to the result observed in unbuffered low-pH agar medium, in which both Col-0 and COM had much better root growth than the *stop1* mutants. Furthermore, the staining of the pH-sensitive dye bromocresol purple showed a significant increase in the rhizospheric pH of Col-0 plants, but not in that of *stop1* mutants (Figure 3C), suggesting that STOP1-conferred H<sup>+</sup> tolerance is associated with an increase in the rhizospheric pH.

To characterize the temporal response of STOP1-regulated rhizospheric pH in response to H<sup>+</sup> stress, we performed a time-course experiment. In the Col-0 rooting medium, we detected a significant increase in pH 3 h after the plants were transferred to low-pH treatment, which represents a fast rhizospheric response; the pH was then further increased over time (Figure 3D). In contrast, the rooting medium pH of the *stop1* mutants did not show any clear alterations during the entire 48 h time course.

### STOP1 is required for induction of H<sup>+</sup> depletion under low-pH conditions

The above findings led us to investigate how STOP1 affects the spatial feature of H<sup>+</sup> depletion by roots using a noninvasive micro-test technique. Low pH clearly induced H<sup>+</sup> influx in Col-0 roots compared with neutral-pH conditions, with an induction that was much greater in the meristematic and elongation zones than in the maturation zone (Figure 3E). Nevertheless, the low pH-induced H<sup>+</sup> influx in all of the tested root zones was substantially suppressed in the *stop1* mutants, indicating that STOP1 acts to enhance H<sup>+</sup> depletion by roots in response to H<sup>+</sup> stress, thereby increasing the rhizospheric pH. The uptake of Evans blue is an indicator of the loss of plasma membrane (PM) integrity (Baker and Mock, 1994). Interestingly, the H<sup>+</sup>-stressed *stop1* had stronger staining of Evans blue in the root tips, including meristematic and elongation zones, in contrast to an almost undetectable staining in the Col-0 roots (Supplemental Figure S5). These results indicate that the meristematic and elongation zones are key sites for STOP1 to avoid H<sup>+</sup> toxicity, which is correlated with the spatial pattern of STOP1-regulated H<sup>+</sup> depletion.

The PM H<sup>+</sup>-ATPase pumps H<sup>+</sup> from the cytosol to the extracellular space. Therefore, we explored whether a higher H<sup>+</sup> influx in Col-0 than in *stop1* under low-pH conditions

was associated with a lower expression level of H<sup>+</sup>-ATPase genes in Col-0. Eleven PM H<sup>+</sup>-ATPase members (AHA1-11) were characterized in Arabidopsis plants (Falhof et al., 2016; Pacifici et al., 2018). The expression of *AHA6* and *AHA9* was undetectable under our experimental conditions. Unexpectedly, low pH upregulated the expression of *AHA3*, *AHA4*, and *AHA7* in Col-0 but not in *stop1* mutants; however, low pH had little effect on the other five AHAs in both Col-0 and *stop1* plants (Supplemental Figure S6). This result refutes our above hypothesis that the enhanced H<sup>+</sup> influx by roots due to STOP1 is associated with a downregulation of H<sup>+</sup>-ATPase genes.

### STOP1 improves NO<sub>3</sub><sup>-</sup> acquisition in response to H<sup>+</sup> stress

The question arises as to how STOP1 improves H<sup>+</sup> influx by roots to increase rhizospheric pH in response to H<sup>+</sup> stress. Previous studies have demonstrated that the uptake of NO<sub>3</sub><sup>-</sup> by roots is accompanied by the depletion of extracellular H<sup>+</sup>, which alkalinizes the rhizosphere (Marschner, 1995; Fang et al., 2016). In this context, we hypothesized that both STOP1-improved H<sup>+</sup> tolerance and NUE may be linked to an increase in root NO<sub>3</sub><sup>-</sup> acquisition. Thus, we first compared the effects of different NO<sub>3</sub><sup>-</sup> supplies on root elongation between Col-0 and *stop1* plants. Three NO<sub>3</sub><sup>-</sup> concentrations (0.1, 6, and 24 mM) were used. In the low-pH treatments with 0.1-mM NO<sub>3</sub><sup>-</sup>, the root growth of Col-0 was severely inhibited, and it did not differ from that of the *stop1* mutants. This contrasted to the results observed for supplementation with 6-mM NO<sub>3</sub><sup>-</sup>, in which Col-0 showed much greater root growth than the *stop1* mutants (Figure 4). A similar result was also obtained in the above low NO<sub>3</sub><sup>-</sup> medium with an increased NH<sub>4</sub><sup>+</sup> supplementation (6 mM) under low-pH conditions (Supplemental Figure S7). These results suggest that STOP1-conferred H<sup>+</sup> tolerance depends on adequate NO<sub>3</sub><sup>-</sup> supplementation. However, when the NO<sub>3</sub><sup>-</sup> concentration in the low-pH treatment increased to 24 mM, the root growth of *stop1* mutants was markedly improved due to a significant increase in rhizospheric pH (Figure 4; Supplemental Figure S8). Consequently, their root elongation was similar to that of Col-0, indicating that excessive NO<sub>3</sub><sup>-</sup> supplementation completely counteracted the destruction of H<sup>+</sup> tolerance due to the loss of function of STOP1. These findings suggest that STOP1-conferred H<sup>+</sup> tolerance is likely associated with NO<sub>3</sub><sup>-</sup> acquisition by roots.

Therefore, we compared the NO<sub>3</sub><sup>-</sup> uptake rate by the roots of the Col-0 and *stop1* mutants under different pH conditions with 6-mM NO<sub>3</sub><sup>-</sup> supplementation. The root NO<sub>3</sub><sup>-</sup> uptake rate of Col-0 in the low-pH treatment was approximately 2.1-fold higher than that in the neutral pH treatment (Figure 4C). Although the root NO<sub>3</sub><sup>-</sup> uptake rate of *stop1* mutants was also slightly increased in response to low pH, the increase was lower than that of Col-0, suggesting that STOP1 is involved in H<sup>+</sup> stress-induced NO<sub>3</sub><sup>-</sup> uptake. A recent study showed that the *stop1* mutants had

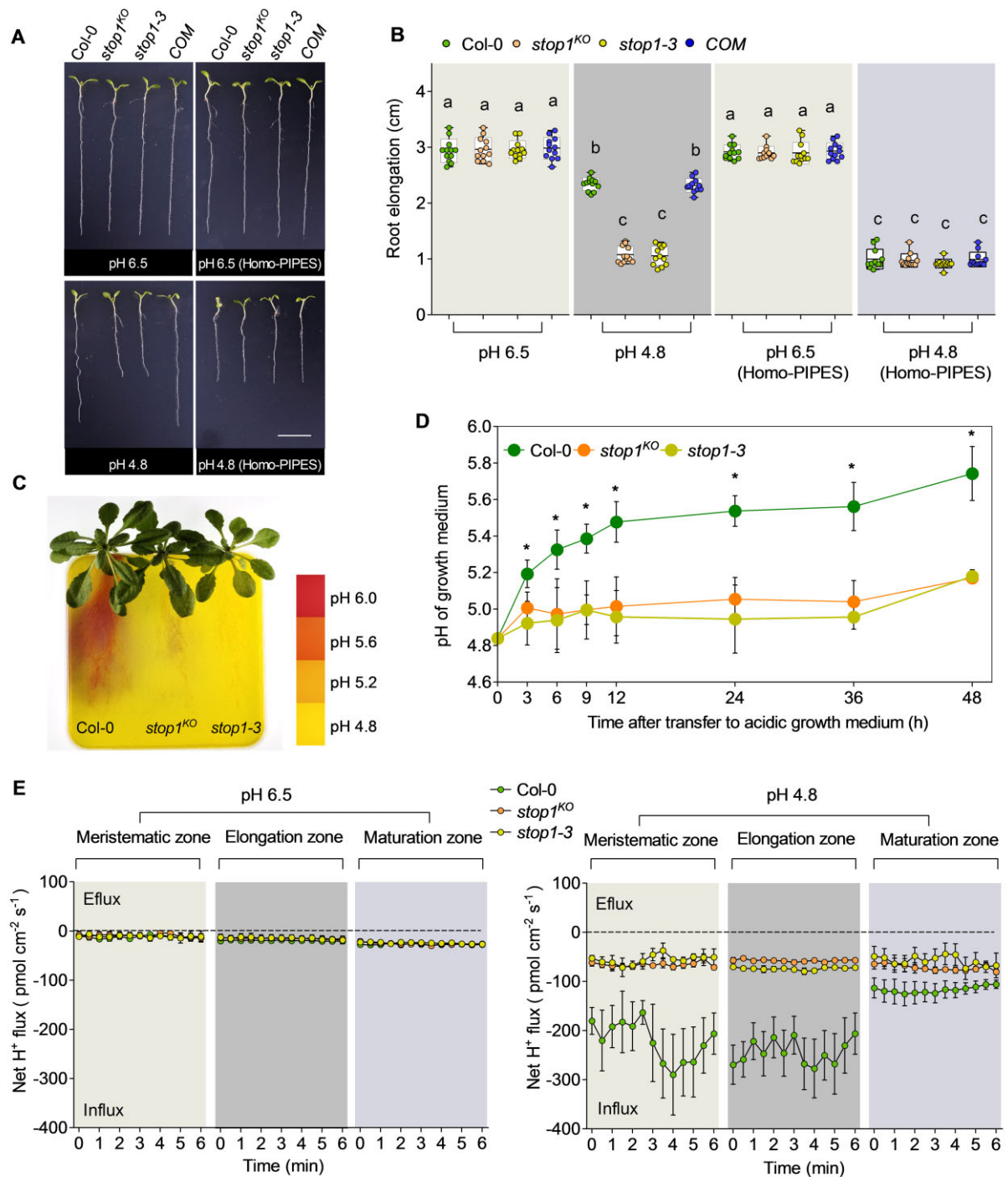


**Figure 3** STOP1-conferred H<sup>+</sup> tolerance depends on an increase in rhizospheric pH. **A** and **B**, Growth of Col-0, *stop1*, and *pSTOP1::GFP-STOP1/stop1<sup>KO</sup>* transgenic plants (COM) in agar media with or without pH buffer. The 3-day-old Arabidopsis seedlings were transferred to a neutral- or low-pH medium with or without 0.75-mM Homo-PIPES for 3 days. Scale bar: 1 cm. Data are presented as the mean  $\pm$  SD of 12 seedlings. The whiskers indicate the minimum and maximum values; the boxes are presented as the mean  $\pm$  SD of 12 seedlings. **C**, Visualization of rhizospheric alkalinization by bromocresol purple staining for 12 h in basal agar media with an initial pH of 4.8. The 5-week-old seedlings were pre-treated at pH 4.8 hydroponically for 1 day before bromocresol purple staining. **D**, Time course of pH alterations in the rooting medium. Plants were grown hydroponically for 5 weeks before being transferred to an acidic growth medium (initial pH = 4.8). Data are presented as the mean  $\pm$  SD of four biological replicates. **E**, H<sup>+</sup> flux measured in different root zones. The 3-day-old seedlings were transferred to a neutral- or low-pH medium for 1 day. Each data point represents the average of the net H<sup>+</sup> flux over 30 s. Data are presented as the mean  $\pm$  SEM of six biological replicates per line and condition. Each experiment was repeated independently three times with similar results, and a representative experiment is shown. Different letters in (**B**) indicate significant differences between means ( $P < 0.05$ ; multiway ANOVA with Tukey's multiple comparisons test). Asterisks in (**D**) indicate significant differences compared with Col-0 ( $*P < 0.05$ ; one-way ANOVA with Tukey's multiple comparisons test).



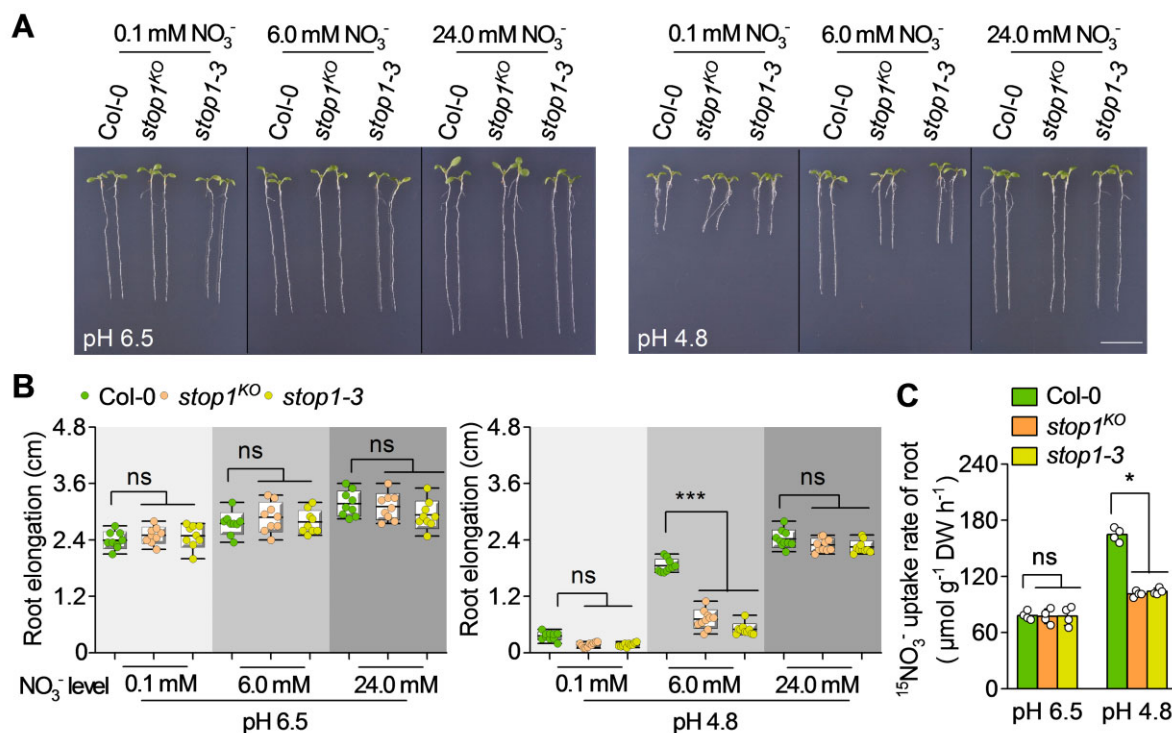


**Figure 4** Mutation of *STOP1* inhibits the stimulation of nitrate uptake by low pH. **A** and **B**, Growth of Col-0 and *stop1* mutants in the medium supplemented with various doses of nitrate. The 3-day-old Arabidopsis seedlings were transferred to neutral- or low-pH medium with several doses of KNO<sub>3</sub> (0.1, 6, and 24 mM). The resulting differences in K concentrations were balanced by adjusting the K<sub>2</sub>SO<sub>4</sub> concentration. The growth of plants was observed and measured 3 days after treatments. Scale bar: 1 cm. The whiskers indicate the minimum and maximum values; the boxes are presented as the mean ± SD of 10 seedlings. **C**, H<sup>+</sup> stress-stimulated nitrate uptake is decreased by the loss of *STOP1* function. 7-day-old Arabidopsis seedlings were pre-treated in the neutral- or low-pH medium for 1 day. The rate of <sup>15</sup>NO<sub>3</sub><sup>-</sup> uptake by roots was measured over 30 min using 6-mM <sup>15</sup>KNO<sub>3</sub> (atom % <sup>15</sup>N, 99%). Data are mean ± SD of four biological replicates. Each experiment was repeated independently three times with similar results, and a representative experiment is shown. Asterisks indicate significant differences between genotypes with the same treatment using two-way ANOVA followed by Tukey's multiple comparison test (\**P* < 0.05; \*\**P* < 0.01; ns, nonsignificant).

higher NH<sub>4</sub><sup>+</sup> uptake than the Col-0 plants in a medium with NH<sub>4</sub><sup>+</sup> as the sole N source (Tian et al., 2021), while NH<sub>4</sub><sup>+</sup> uptake usually causes rhizosphere acidification. We therefore compared the root NH<sub>4</sub><sup>+</sup> uptake rate between Col-0 and *stop1* mutants. In the media of our current study in which 6-mM NO<sub>3</sub><sup>-</sup> and 2-mM NH<sub>4</sub><sup>+</sup> were used as the N source, these plant lines did not differ in the rate of root NH<sub>4</sub><sup>+</sup> uptake under either low or neutral pH conditions (Supplemental Figure S9). These results further indicate that both *STOP1*-improved H<sup>+</sup> tolerance and NUE may be associated with the induction of NO<sub>3</sub><sup>-</sup> uptake rather than the regulation of NH<sub>4</sub><sup>+</sup> uptake.

#### Induction of *NRT1.1* by H<sup>+</sup> stress requires the action of *STOP1*

Currently, six *NRTs* have been characterized as being involved in NO<sub>3</sub><sup>-</sup> uptake in Arabidopsis plants, including *NRT1.1*, *NRT1.2*, *NRT2.1*, *NRT2.2*, *NRT2.4*, and *NRT2.5* (Wang et al., 2012; Lezhneva et al., 2014). To investigate the molecular basis underlying the induction of root NO<sub>3</sub><sup>-</sup> uptake by *STOP1* in response to H<sup>+</sup> stress, we analyzed the expression of these six *NRTs* in the roots of Col-0 and *stop1* mutants under different pH conditions (Figure 5A). *NRT2.5*

was undetectable under our experimental conditions, most likely because this gene is predominantly highly expressed in N-starved adult plants (Lezhneva et al., 2014). The expression of the other five *NRTs* did not show any differences between the Col-0 and *stop1* mutants at a neutral pH. When the seedlings were grown at low pH, only *NRT1.1* was differentially regulated due to the loss of *STOP1* function, as in Col-0 it was markedly upregulated by approximately sevenfold compared with that in the neutral-pH treatment, but in the *stop1* mutants it was barely affected (Supplemental Figure S10). Given that *NRT1.1* contributes to the majority of root NO<sub>3</sub><sup>-</sup> uptake under adequate NO<sub>3</sub><sup>-</sup> supplementation (Huang et al., 1996; Liu et al., 1999), failure in the induction of *NRT1.1* may explain why the *stop1* mutants did not markedly upregulate root NO<sub>3</sub><sup>-</sup> uptake, similar to Col-0 plants, in response to H<sup>+</sup> stress.

We subsequently investigated how *STOP1* affected the spatial features of *NRT1.1* expression in roots in response to H<sup>+</sup> stress. Although lowering the pH in growth media had little effect on the transcript level of *STOP1* in Col-0 roots, it increased the nucleus-localized GFP-*STOP1* in the root epidermal cells of *pSTOP1::GFP-STOP1* transgenic plants (Figure 5B; Supplemental Figure S11). This result is

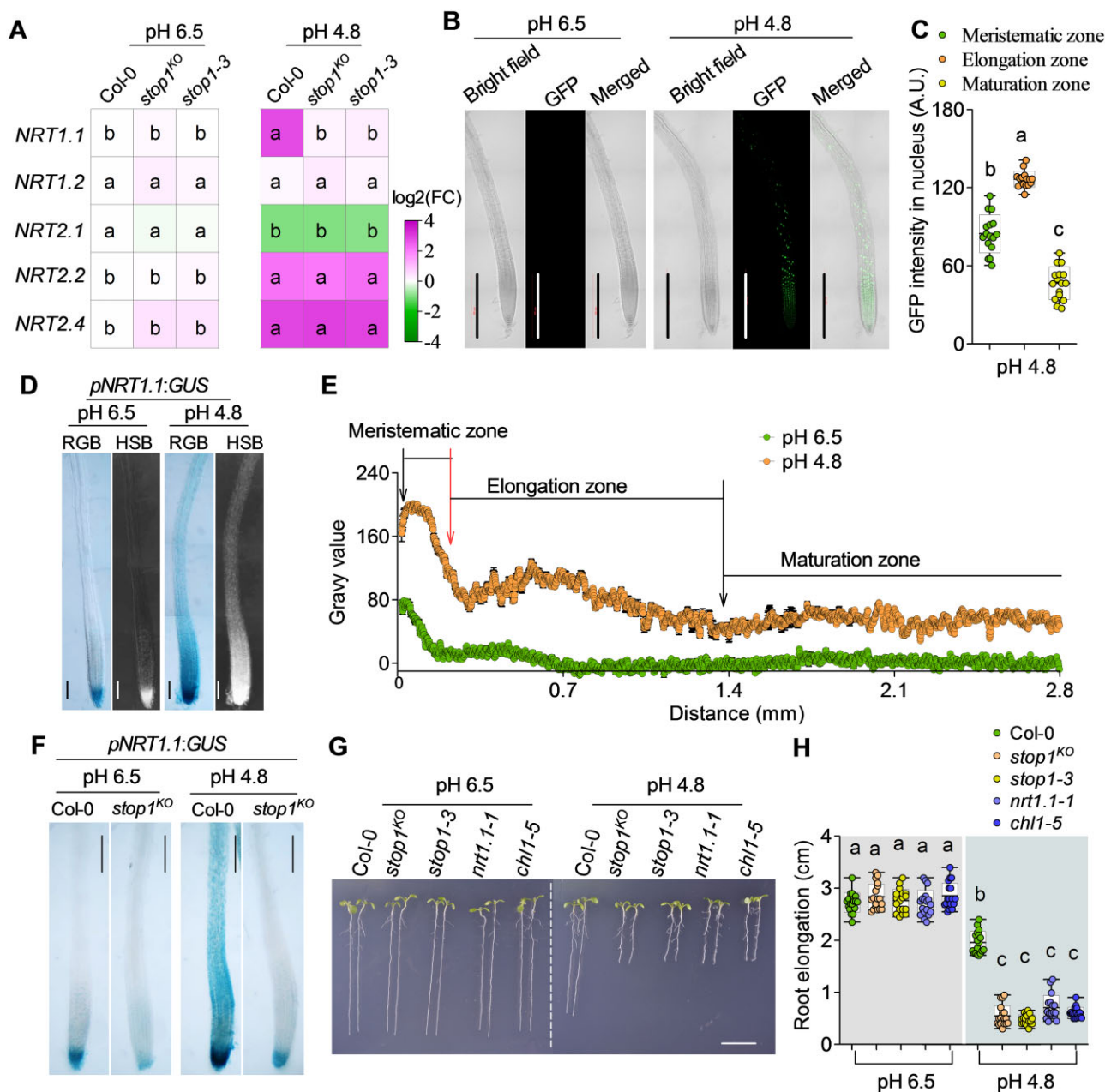


**Figure 5** Mutation of *STOP1* abolishes low pH-mediated *NRT1.1* induction. **A**, RT-qPCR analyses of nitrate uptake-related genes in the roots of wild-type and *stop1* mutants. The heat map shows the mean  $\log_2$ -transformed relative expression levels from the five biological replicates. Raw data on the relative gene expression are shown in [Supplemental Figure S10](#). **B**, Images of GFP-STOP1 in *pSTOP1:GFP-STOP1/stop1<sup>KO</sup>* seedlings. Scale bar: 0.5 mm. **C**, Quantification of fluorescence intensities of GFP-STOP1 in different root zones. **D**, Image of GUS staining and its hue saturation brightness (HSB) mode in *pNRT1.1:GUS/Col-0* seedlings. Scale bar: 0.3 mm. **E**, Profile of quantified GUS intensity measured in the HSB image. **F**, Comparison of GUS expression in *pNRT1.1:GUS/Col-0* and *pNRT1.1:GUS/stop1<sup>KO</sup>* seedlings. Scale bar: 0.2 mm. **G** and **H**, *STOP1*-null mutants *stop1<sup>KO</sup>* and *stop1-3*, and *NRT1.1*-null mutants *nrt1.1-1* and *chl1-5* had a very similar hypersensitive phenotype to  $H^+$  stress. Scale bar: 1 cm. The 3-day-old *Arabidopsis* seedlings were transferred to a neutral- or low-pH medium. The growth of the plants was observed and measured 3 days after treatment, whereas the other experiments were performed 1 day after treatment. The whiskers indicate the minimum and maximum values; the boxes are presented as the mean  $\pm$  SD of 16 seedlings in (**C**) and of 18 seedlings per line and condition in (**H**). All experiments were independently repeated at least three times with similar results, and one representative experiment is shown. Different letters indicate significant differences between means, as determined by Tukey's multiple comparisons test at  $P < 0.05$  (two-way ANOVA in (**A**) and (**H**); one-way ANOVA in (**C**)).

consistent with the findings of previous studies (Iuchi et al., 2007; Godon et al., 2019). In addition, the increased accumulation of GFP-STOP1 in the nucleus of root cells at low pH was independent of the level of  $NO_3^-$  supplementation in

the growth media (Supplemental Figure S12). Quantification of fluorescence intensities showed that the abundance of GFP-STOP1 in roots under low pH stress was greater in the meristematic and elongation zones than in the maturation



zone (Figure 5C). The root expression patterns of *NRT1.1* in *pNRT1.1:GUS* transgenic plants were also examined by GUS staining. In comparison with neutral pH treatment, low pH treatment increased *NRT1.1* expression level in all tested root zones, with a greater increase in the meristematic and elongation zones than in the maturation zone (Figure 5, D and E), thus showing a spatial pattern similar to that of STOP1. Nevertheless, the greatest GUS staining was in the meristematic zone, most likely due to the high pH-independent background expression of *NRT1.1* in this zone. Then, the *pNRT1.1:GUS* transgenic line was crossed with the *stop1*<sup>KO</sup> mutants to generate *pNRT1.1:GUS/stop1*<sup>KO</sup> plants, and GUS staining demonstrated that the low pH-established spatial expression pattern of *NRT1.1* in roots, especially in the zones of the root tip, required the action of STOP1 (Figure 5F).

Combined with the fact that the root tip is the most sensitive root zone to H<sup>+</sup> stress (Figure 3; Supplemental Figure S5), the above results suggest that both the abundance and spatial distribution of *NRT1.1* transcription in roots are optimized by STOP1 to effectively enhance H<sup>+</sup> depletion and create a favorable rhizospheric pH for plant adaptation to H<sup>+</sup> stress. The *NRT1.1*-null (*nrt1.1-1* and *chl1-5*), and the *stop1* mutants had a similar hypersensitive phenotype to H<sup>+</sup> stress (Figure 5, G and H). Furthermore, the *nrt1.1* mutants were stained by Evans blue in the root tip in a manner similar to that in the *stop1* mutants under low-pH conditions (Supplemental Figure S5). These results support the above hypothesis that the spatial pattern of *NRT1.1* is finely regulated by STOP1 to cope with H<sup>+</sup> stress.

### STOP1 binds directly to the *NRT1.1* promoter

We examined whether STOP1 binds directly to the promoter of *NRT1.1* using a *Nicotiana benthamiana* leaf transactivation assay. The full-length promoter (4.5 kb) of *NRT1.1* was divided into three segments (P1, P2, and P3; Figure 6A), each of which was fused with a luciferase gene (*LUC*; Supplemental Figure S13A). When an effector STOP1-expressing construct (expression driven by the CaMV35S promoter) was co-transformed with each of these three reporter constructs individually, only the P1-derived luciferase activity was higher than that when the empty vector (EV) control was co-transformed (Figure 6B). Subsequently, the P1 segment was divided into four shorter segments. The co-expression of these shorter-segment constructs with the STOP1 effector yielded detectable P1-2-derived LUC signals, but no detectable signal from the other three segments, indicating that STOP1 activates the *NRT1.1* promoter by binding to the region between −4,137 bp and −3,615 bp from ATG (Figure 6, C and D). An analysis based on the Plant Cistrome Database (O'Malley et al., 2016) also identified a putative binding site for STOP1 in the P1-2 segment of the *NRT1.1* promoter, which is in high agreement with previously published binding motifs (Supplemental Figure S14; Tokizawa et al., 2015; Zhang et al., 2019; Sadhukhan et al., 2019; Tokizawa et al., 2021).

Chromatin immunoprecipitation (ChIP) experiments were carried out with GFP-STOP1-expressing plants to explore

whether STOP1 binds to the P1-2 segment of the *NRT1.1* promoter in vivo. After ChIP with anti-GFP antibody, the enrichment of two *NRT1.1* promoter fragments in the immunoprecipitant (Figure 6E) was assessed by qPCR using two primer pairs (Supplemental Data Set S1). GFP-STOP1 was significantly enriched at the promoter region of the P1-2-A fragment, but not P1-2-B, compared to the wild-type control (Figure 6F). We also compared the binding of STOP1 with the wild-type and mutated forms of the P1-2-A segment using a *N. benthamiana* leaf transactivation assay. As expected, only the P1-2-A wild-type-derived LUC/REN ratio and luciferase activity were higher than that when the EV control was co-transformed (Figure 6G; Supplemental Figure S13B). Next, we purified His-TF-tagged STOP1 and performed electrophoretic mobility shift assays (EMSA) with the biotin-labeled *NRT1.1* promoter DNA (35 bp within P1-2-A). As shown in Figure 6H, His-TF-STOP1 was able to bind to biotin-labeled wild-type DNA, and the binding activity was reduced by the addition of an unlabeled competitor. Furthermore, the binding capacity of His-TF-STOP1 to mutated DNA probes was also greatly diminished (Figure 6H). Taken together, these results demonstrate that STOP1 directly binds to the *NRT1.1* promoter, which supports the activation of *NRT1.1* transcription in response to acidic stress.

### *NRT1.1* acts downstream of STOP1 in NO<sub>3</sub><sup>−</sup> uptake activation and root growth maintenance under low-pH conditions

Since *nrt1.1* mutants developed a H<sup>+</sup>-hypersensitive phenotype similar to *stop1* mutants and *NRT1.1* is a direct target gene of STOP1 (Figures 5 and 6), we further explored whether STOP1 and *NRT1.1* function in the same pathway in response to H<sup>+</sup> stress. To this end, we generated a *stop1 nrt1.1* double mutant by crossing the *nrt1.1-1* and *stop1*<sup>KO</sup> mutants (Supplemental Figure S15). Under neutral pH conditions, the *nrt1.1-1* and *stop1 nrt1.1* plants had a lower root NO<sub>3</sub><sup>−</sup> uptake than Col-0 and *stop1*<sup>KO</sup> (Figure 7), probably because the latter two plants still have a basal expression of *NRT1.1* in roots (Supplemental Figure S10). However, low-pH treatment in the agar medium failed to induce root NO<sub>3</sub><sup>−</sup> uptake of *stop1 nrt1.1* double mutant in a manner similar to that of the *nrt1.1-1* mutants (Figure 7A). A similar result was observed in plants grown in hydroponic media (Supplemental Figure S16). Furthermore, *stop1 nrt1.1* had a root growth phenotype similar to that of *nrt1.1-1* and *stop1*<sup>KO</sup> in the low-pH agar medium (Figure 7, B and C). These results suggest that STOP1 and *NRT1.1* function in the same pathway mediating NO<sub>3</sub><sup>−</sup> uptake activation and H<sup>+</sup> tolerance under low pH. Because STOP1 directly activates *NRT1.1* transcription by binding to its promoter, we hypothesized that *NRT1.1* is located downstream of STOP1 to induce H<sup>+</sup>-coupled NO<sub>3</sub><sup>−</sup> uptake by roots under low-pH conditions, thereby creating a favorable rhizosphere pH for root growth.

To test this hypothesis, we used a constitutive promoter, CaMV 35S, to restore *NRT1.1* expression in the roots of

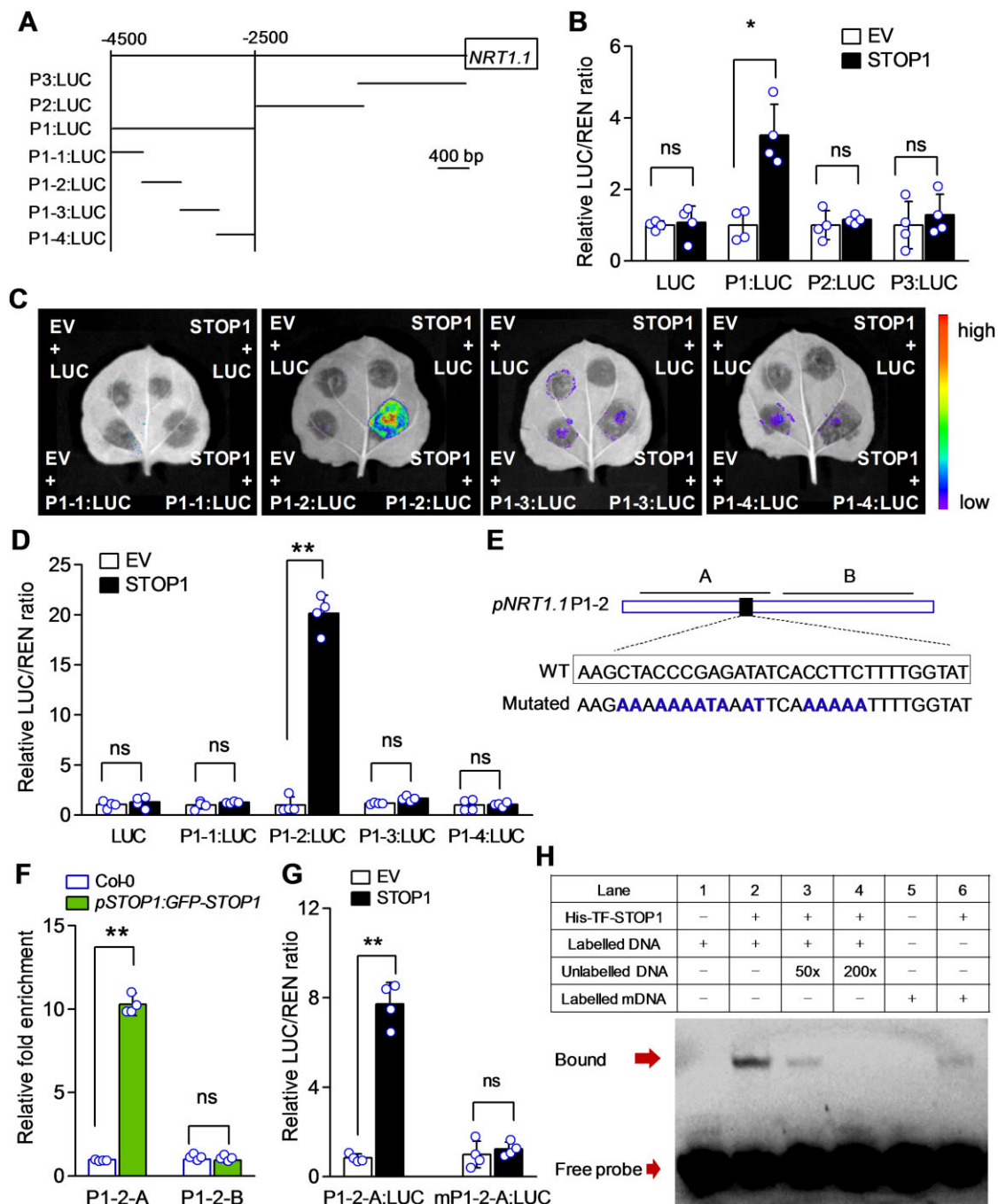


**Figure 6** STOP1 directly binds to the *NRT1.1* promoter. **A**, Diagram of *NRT1.1*. P1–P3 and P1-1 to P1-4 are the fragments used in the transient dual-luciferase assays. **B–D**, The *in vivo* interactions between STOP1 and the fragments of *NRT1.1* via transient dual-luciferase assays in *N. benthamiana* leaves. The EV pCambia1300 was used as a negative control (set as 1). Effector and reporter constructs were co-transformed into *N. benthamiana* leaves for 48 h, after which the ratio of firefly and Renilla luciferase activities were measured and visualized. Data are presented as the mean  $\pm$  SD of 4 biological replicates. **E**, Diagram of the P1-2 fragments. The site of *NRT1.1* promoter (–3963 to –3994 bp from ATG) potentially targeted by STOP1 was indicated in a box. Blue letters represent the mutations in the mutant P1-2-A fragment or the mutant sequence used in EMSA. **F**, ChIP-qPCR analysis of STOP1 DNA-binding activity to the P1-2-A and P1-2-B fragments. Chromatin was isolated from *pSTOP1:GFP-STOP1/stop1<sup>KO</sup>* and Col-0 with 1 day low-pH treatment and immunoprecipitated with GFP antibody. The enrichment of *NRT1.1* promoter fragments in the immune precipitant was determined by qPCR, and fold enrichment represents the immunoprecipitation efficiency in the GFP-SOP1 transgenic plants normalized to that in the Col-0 plants. Data are presented as the mean  $\pm$  SD of three samples, each with three technical replicates. **G**, The *in vivo* interactions between STOP1 and the WT- and mutated-form of P1-2-A fragments of *NRT1.1* via transient dual-luciferase assays in *N. benthamiana* leaves. Data are presented as the mean  $\pm$  SD of four biological replicates. **H**, EMSA of recombinant His-TF-STOP1 protein binding to the P1-2-A fragment in the *NRT1.1* promoter. The biotin-labeled WT fragment (the sequence in the box of (E)) or its mutated version was incubated with 1.5  $\mu$ g of purified His-TF-STOP1 proteins. All experiments were independently repeated at least twice with similar results, and a representative experiment is shown. Asterisks indicate significant differences ( $^*P < 0.05$ ;  $^{**}P < 0.01$ ; ns, non-significant; one-way ANOVA with Tukey's multiple comparisons test).

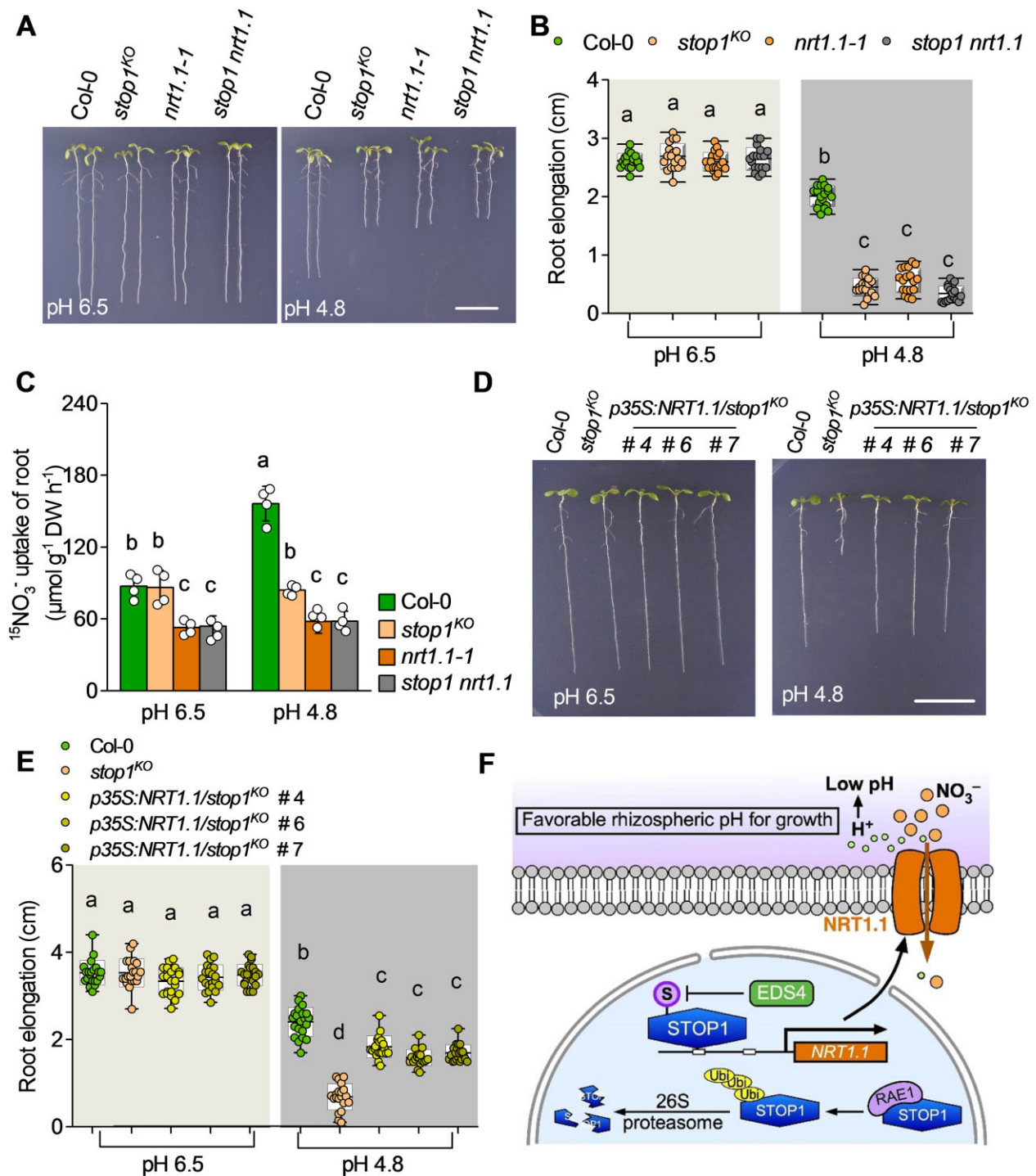


**Figure 7** NRT1.1 functions downstream of STOP1 in response to low pH. A and B, Comparison of root growth between single and double mutants of *stop1* and *nrt1.1*. C, Comparison of nitrate uptake rates between single and double mutants of *stop1* and *nrt1.1*. Seedlings were treated as described in Figure 4C. Data are presented as the mean  $\pm$  SD of four biological replicates per line and condition. D and E, Growth recovery of *stop1* mutant by expressing NRT1.1 under the control of the *CaMV* 35S promoter. The whiskers indicate the minimum and maximum values; the boxes are presented as the mean  $\pm$  SD ( $n = 10$  seedlings per line and condition in (C);  $n = 19$ – $21$  seedlings per line and condition in (E)). The 3-day-old plants were transferred to a neutral- or low-pH medium for 3 days. Scale bar: 1 cm. All experiments were repeated independently at least three times with similar results, and one representative experiment is shown. Different letters indicate significant differences between means ( $P < 0.05$ ; two-way ANOVA with Tukey's multiple comparisons test). F, Proposed model for STOP1-NRT1.1 in improving plant adaptation to acidity. The high dose of H<sup>+</sup> in the acidic soils stimulates STOP1 accumulation in the nucleus, activating the expression of nitrate transporter gene NRT1.1 by binding to its promoter. Increased NRT1.1 expression improves the H<sup>+</sup>-coupled NO<sub>3</sub><sup>-</sup> uptake by roots, which enhances the depletion of rhizospheric H<sup>+</sup>, thus creating a favorable rhizospheric pH for plant growth.



*stop1*<sup>KO</sup> under low-pH conditions. Although the *p35S:NRT1.1/stop1*<sup>KO</sup> transgenic lines had higher *NRT1.1* expression in roots than Col-0 (Supplemental Figure S17A), their root NO<sub>3</sub><sup>-</sup> uptake rates were slightly lower than those of Col-0 (Supplemental Figure S17B). This may be because CaMV 35S is a constitutive promoter that does more than just control *NRT1.1* expression in root epidermis–cortex cells. Even so, the root growth of *stop1*<sup>KO</sup> was almost fully restored by transformation with the *p35S:NRT1.1* construct under low-pH conditions (Figure 7, D and E), providing direct evidence that *NRT1.1* acts downstream of STOP1 to confer plant H<sup>+</sup> tolerance. Recently, *CBL-INTERACTING PROTEIN KINASE 23* (*CIPK23*) was also shown to be a target gene of STOP1 (Sadhukhan et al., 2019). *CIPK23* phosphorylates *NRT1.1* to regulate its affinity for NO<sub>3</sub><sup>-</sup> uptake (Ho et al., 2009), which prompted us to determine whether the STOP1-*CIPK23* module was also involved in STOP1-conferred H<sup>+</sup> tolerance. However, the root growth of *cipk23* mutants was comparable to that of Col-0 under low-pH conditions (Supplemental Figure S18). This result demonstrated that the STOP1-*CIPK23* module is not involved in H<sup>+</sup> tolerance or its regulation of the affinity of NO<sub>3</sub><sup>-</sup> uptake is not sufficient to create a favorable rhizospheric pH for the adaptation of plants to H<sup>+</sup> stress.

## Discussion

The identification of biological mechanisms underlying the responses of nutrient acquisition and tolerance of plants to H<sup>+</sup> stress is a crucial step in improving nutrient use efficiency and plant production in acidic soils. NO<sub>3</sub><sup>-</sup> is the main absorbable form of N by the roots of plants in agricultural and natural systems (Vidal et al., 2020). The uptake of NO<sub>3</sub><sup>-</sup> by the root is an H<sup>+</sup>-coupled process, that is, the H<sup>+</sup>/NO<sub>3</sub><sup>-</sup> symport across the plasmalemma (Marschner, 1995; Liu et al., 1999; Wang et al., 2012). Based on this H<sup>+</sup>/NO<sub>3</sub><sup>-</sup> symport mechanism and the results of our current study, we proposed a model to explain how plants adapt to acidic conditions (Figure 7F). In this model, the low pH-enriched STOP1 in the nucleus directly activates the expression of *NRT1.1*, by binding to its promoter to stimulate the H<sup>+</sup>-coupled NO<sub>3</sub><sup>-</sup> uptake by *NRT1.1*; subsequently, it enhances the depletion of H<sup>+</sup> in the rhizosphere, ultimately creating a favorable pH environment for root growth.

The transcriptional regulation of *NRT1.1* by STOP1 explains the phenomenon whereby the lowering of pH in growth medium significantly induces *NRT1.1* expression in roots (Tsay et al., 1993). Previous transcriptome comparisons between Col-0 and *stop1* mutants did not find positive regulation of *NRT1.1* by STOP1 in response to acidic stress (Iuchi et al., 2007; Sawaki et al., 2009). This is probably because the plants in that study were grown in a phosphate-eliminated medium, which would significantly downregulate the expression of *NRT1.1* (Wang et al., 2020) and thus counteract the positive regulation by STOP1. *NRT1.1* was the first nitrate transporter identified in NO<sub>3</sub><sup>-</sup> uptake in vascular plants (Tsay et al., 1993; Wang et al., 2018; Vidal et al., 2020). The

expression of *NRT1.1* was markedly higher than that of the other *NRT* genes (Supplemental Figure S10), while the loss of *NRT1.1* function resulted in an ~60% decrease in the uptake rate in the low-pH growth media supplemented with sufficient NO<sub>3</sub><sup>-</sup> (Figure 7; Supplemental Figure S19). Therefore, *NRT1.1* contributed to the majority of root NO<sub>3</sub><sup>-</sup> uptake in response to acidic stress. This contribution allowed STOP1-*NRT1.1* module-regulated NO<sub>3</sub><sup>-</sup> uptake to construct a suitable pH environment in the rhizosphere for roots when they were challenged by acidic conditions (Figure 3). Interestingly, STOP1 primarily activated *NRT1.1* transcription and H<sup>+</sup> depletion in the meristematic and elongation zones, which are the most sensitive to H<sup>+</sup> toxicity parts of the roots (Figures 3 and 5; Supplemental Figure S5). This fine-targeted regulation may allow plants to cope with H<sup>+</sup> toxicity in an energy-efficient way. In this study, we also found that low pH upregulated the expression of *AHA3*, *AHA4*, and *AHA7* in a STOP1-dependent manner (Supplemental Figure S6). Studies indicate that the uptake of NO<sub>3</sub><sup>-</sup> by root cells relies on the activity of PM ATPase and H<sup>+</sup>/NO<sub>3</sub><sup>-</sup> symport into root cells, with the H<sup>+</sup>/NO<sub>3</sub><sup>-</sup> ratio being greater than one (Feng et al., 2020). In this context, although PM H<sup>+</sup>-ATPase generates a maximum of one H<sup>+</sup> per ATP hydrolyzed and pumps H<sup>+</sup> to the extracellular space (Pedersen et al., 2015), upregulation of the above three AHAs in the roots of Col-0 may be a favorable factor for improving *NRT1.1*-mediated NO<sub>3</sub><sup>-</sup> uptake to deplete rhizospheric H<sup>+</sup>.

It is worth noting that excessive NO<sub>3</sub><sup>-</sup> supplementation could effectively improve root growth in an acidic medium by increasing the rhizospheric pH in a STOP1-independent manner (Figure 4; Supplemental Figure S8). The *stop1* mutants still had basal expression of *NRT1.1*, although the level of this basal expression was low (Supplemental Figure S10). Theoretically, a decrease in NO<sub>3</sub><sup>-</sup> uptake due to the loss of STOP1 function in acidic conditions could be compensated for by increasing the nitrate supply, which can increase the NO<sub>3</sub><sup>-</sup> uptake mediated by basal *NRT1.1* expression and other *NRT*s. This assumption was supported by the findings that the NO<sub>3</sub><sup>-</sup> uptake rate was higher in *stop1* mutants than in *nrt1.1* mutants and that the rate was clearly increased in both mutants by an increase in NO<sub>3</sub><sup>-</sup> supply either in neutral or acidic conditions (Figure 7; Supplemental Figure S19). However, because the above NO<sub>3</sub><sup>-</sup> uptake pathways require high NO<sub>3</sub><sup>-</sup> supplementation to effectively improve root growth under acidic conditions, their contribution to plant adaptation to most natural acidic soils should be limited.

Soils normally have pH-buffering capacity. Soils rich in organic matter (OM) often have a higher pH buffering capacity (Aitken et al., 1990; Nelson and Su, 2010). Nevertheless, many studies have shown that, despite the pH buffering capacity of soils, the plants could remarkably change the pH in root-adjacent soils, particularly in rhizospheric soils (Smiley, 1974; Bagayoko et al., 2000; Bravin et al., 2009). An obvious change in rhizospheric pH by plant roots was even

observed in soil with a relatively higher OM content ( $> 3\%$ ; Gijssman, 1990). The spatial restriction of the narrow rhizospheric zone should theoretically enable an intensive flow of  $H^+$  between the soil and roots, which allows roots to effectively regulate the pH in rhizospheric soil. A prolonged growth period of a plant would also permit the roots to cumulatively counter the pH buffering capacity of soils. These factors may explain why the STOP1-NRT1.1 module in Col-0 could effectively improve plant growth in acidic soils (Figure 1A; Supplemental Figure S2). However, the extent of pH change in rhizospheric soil due to  $H^+$  depletion by roots could be affected by soil pH buffering capacity. In this context, a greater pH buffering capacity in acidic soil would lead to a lower efficacy for the STOP1-NRT1.1 module to improve plant growth. This notion was supported by the observation that the normal function of STOP1 in Col-0 did not confer enhanced root growth in an agar medium containing an excellent pH buffer (Figure 3; Supplemental Figure S4).

Because of the enhanced  $NO_3^-$  uptake and improved root growth, the  $H^+$ -stimulated STOP1-NRT1.1 module clearly improved the NUE of Arabidopsis plants in acidic soils (Figures 1 and 4). To satisfy the increasing demand for food, farmers currently apply over 110 Tg of N fertilizers annually to improve crop production, resulting in a growing global demand for N fertilizer in agriculture (Schroeder et al., 2013; Chen et al., 2020). Urea is the most commonly used commercial N fertilizer. In China, urea fertilizers account for nearly 70% of the total N fertilizers used (Zhang et al., 2013). Nevertheless, the excessive application of urea fertilizer not only leads to a low NUE of plants but also aggravates soil acidification, which is a main agronomic and environmental concern (Guo et al., 2010; Jadon et al., 2018; Guo et al., 2020; Kissel et al., 2020). After its application to soils, urea is hydrolyzed to  $NH_3$ , which is subsequently nitrified into  $NO_3^-$  and  $H^+$  (Sigurdarson et al., 2018). The loss of  $NH_3$  volatilization and  $NO_3^-$  leaching are the greatest contributors to N loss under most soil conditions (Jadon et al., 2018), while the  $H^+$  generated from nitrification significantly accelerates soil acidification (Shi et al., 2019). Therefore, increasing urea-N recovery by plants, reducing  $NH_3$  volatilization and  $NO_3^-$  leaching, and removing nitrification-generated  $H^+$  remain the biggest agronomic challenges associated with the use of urea in global agriculture practices. A low pH in acidic soils slows microbe-mediated nitrification (Li et al., 2018). Removing rhizospheric  $H^+$  by the plant STOP1-NRT1.1 module could reduce  $NH_3$  volatilization by accelerating nitrification in the rhizosphere via the creation of a favorable pH. In addition, either the enhanced uptake of  $NO_3^-$  by the roots due to the STOP1-NRT1.1 module or the spatial restriction of the rhizosphere in accelerated nitrification could also favor a reduction in  $NO_3^-$  leaching losses. Therefore, the promising prospects for the STOP1-NRT1.1 module and its homologs in solving the aforementioned agronomic challenges from the use of urea should be the focus of future studies.

In summary, the current study elucidates that the STOP1-NRT1.1 is a key module for plants to create a favorable rhizospheric pH for their adaptation to acidic conditions by improving the  $H^+$ -coupled  $NO_3^-$  uptake by roots (Figure 7F). Our findings show that the construction of favorable rhizospheric pH by plants per se could be an efficient strategy for plants to compensate for not being able to escape when challenged by  $H^+$  stress in acidic soils. It is worth noting that the transcript level of STOP1 was not responsive to low pH (Supplemental Figure S11), suggesting a post-transcriptional activation of STOP1 upon  $H^+$  stress. Although the post-translational regulation via RAE1-involved ubiquitin-26S proteasome and ESD4-catalyzed deSUMOylation pathways has been demonstrated to act in the  $Al^{3+}$  stress-induced STOP1 protein accumulation (Zhang et al., 2019; Fang et al., 2020), the basis of signaling for nucleus-localized STOP1 enrichment linked to  $H^+$  stress still needs to be elucidated in future studies.

## Materials and Methods

### Plant material

The *A. thaliana* plants used in this work were all from Columbian (Col-0) background. The various mutants were *stop1<sup>KO</sup>* (SLAK\_114108), *stop1-3* (a point mutant in which the His 352 of STOP1 is replaced with Try 352; Zhang et al., 2019), *nrt1.1-1* (SALK\_097431), *chl1-5* (Tsay et al., 1993), *almt1<sup>KO</sup>* (SALK\_009629), *lks1-2* (Xu et al., 2006), and *lks1-3* (SALK\_036154). The *pSTOP1:GFP-STOP1/stop1<sup>KO</sup>* transgenic line (#B10) used in this study has been described in Balzergue et al. (2017). The *stop1 nrt1.1* double mutants were generated by crossing *stop1<sup>KO</sup>* with *nrt1.1-1*, and homozygous lines were identified by PCR. We also crossed *pNRT1.1:GUS* with *stop1<sup>KO</sup>*, and the homozygous lines were identified by PCR. The primers used are shown in Supplemental Data Set S1.

To generate *p35S:NRT1.1*, the coding region of *NRT1.1* was amplified by PCR and inserted into pCambia1300 using the SacI and BamHI restriction sites. The construct was then introduced into the *Agrobacterium* strain GV3101. The *stop1<sup>KO</sup>* mutants were used as recipients for *Agrobacterium*-mediated transformation to generate transgenic Arabidopsis. The primers used for generating the various clones are also listed in Supplemental Data Set S1. All constructs were confirmed by sequencing. Homozygous T3 plants were used in subsequent experiments.

### Plant growth condition

Three days of stratification were conducted at 4°C before sowing the seeds. Surface-sterilized Arabidopsis seeds were sown on basal agar medium containing  $KNO_3$  (6 mM),  $(NH_4)_2SO_4$  (1 mM),  $NaH_2PO_4$  (1 mM),  $MgSO_4$  (500  $\mu$ M),  $CaCl_2$  (1 mM),  $H_3BO_3$  (10  $\mu$ M),  $MnSO_4$  (0.5  $\mu$ M),  $ZnSO_4$  (0.5  $\mu$ M),  $CuSO_4$  (0.1  $\mu$ M),  $(NH_4)_6Mo_7O_{24}$  (0.1  $\mu$ M), Fe-EDTA (25  $\mu$ M), 0.8% agar (Sigma-Aldrich, A1296), 1% sucrose at pH 6.5 under controlled environmental conditions at 22°C–24°C, 100  $\mu$ mol  $m^{-2} s^{-1}$  (WEGA WEN-8 LED cool-

white light lamp, Weifang, China), and a 14-h light/10-h dark photoperiod cycle. Then, the 3-day-old plants were used for phenotype analysis in the above basal agar medium with an initial pH of either 4.8 or 6.5, and various doses of Homo-PIPES were used for the buffering assay, as indicated in the figure legends. To analyze the specific root growth in response to different N sources, the media were supplemented with appropriate concentrations of  $\text{KNO}_3$  or  $(\text{NH}_4)_2\text{SO}_4$ , as described in the figure legends. The resulting differences in K concentrations were balanced by adjusting the  $\text{K}_2\text{SO}_4$  concentration.

For soil culture, the plants were grown in square pots (6 cm in length and height) containing either acidic or neutral soil. The basic physicochemical properties of the soils used in this study are shown in the [Supplemental Table S1](#). Five-day-old plants were transferred to the soil systems. The pots were weighed and watered every day to maintain a maximum water retention capacity of 55%–65% for the soil. The plants in each pot were fertilized weekly with an appropriate amount of urea or  $\text{Ca}(\text{NO}_3)_2$  dissolved in 13.5 mL of medium, as indicated in the figure legends. The composition of other nutrients in the fertilizing medium for the soil systems was as follows (1 L):  $\text{NaH}_2\text{PO}_4$  (2 mM),  $\text{K}_2\text{SO}_4$  (2 mM),  $\text{MgSO}_4$  (500  $\mu\text{M}$ ),  $\text{CaCl}_2$  (1 mM),  $\text{H}_3\text{BO}_3$  (10  $\mu\text{M}$ ),  $\text{MnSO}_4$  (0.5  $\mu\text{M}$ ),  $\text{ZnSO}_4$  (0.5  $\mu\text{M}$ ),  $\text{CuSO}_4$  (0.1  $\mu\text{M}$ ),  $(\text{NH}_4)_6\text{Mo}_7\text{O}_{24}$  (0.1  $\mu\text{M}$ ), and Fe-EDTA (25  $\mu\text{M}$ ). Plants were harvested after four rounds of fertilization.

### Measurement of $\text{H}^+$ depletion, $\text{NO}_3^-$ uptake, and N content

A noninvasive microelectrode ion flux measurement system (ipa-2; AE, USA) was used to measure the net fluxes of  $\text{H}^+$ , as previously described ([Zhu et al., 2019](#)). Briefly, 3-day-old seedlings were grown in agar medium with a pH of 6.5 or 4.8 for 1 day. Then, the  $\text{H}^+$  fluxes in the epidermal root cells were measured along the root axis in the meristematic, elongation, and maturation zones using an  $\text{H}^+$ -selective microelectrode.

For the assays of  $\text{NO}_3^-$  and  $\text{NH}_4^+$  uptakes, 7-day-old seedlings were pre-treated in agar medium with a pH of 6.5, or 4.8, for 1 day. The plants were washed with 0.05-mM  $\text{CaSO}_4$  for 1 min and then transferred to a medium in which  $\text{KNO}_3$  or  $(\text{NH}_4)_2\text{SO}_4$  was replaced with  $\text{K}^{15}\text{NO}_3$  (atom %  $^{15}\text{N}$ , 99%) or  $(\text{NH}_4)_2\text{SO}_4$  (atom %  $^{15}\text{N}$ , 99%), respectively, for 30 min under the same conditions used for pre-culturing seedlings. The plants were washed with 0.5-mM  $\text{CaSO}_4$  for 1 min, after which each plant was separated into shoots and roots, and the organs were dried at 65°C for 3 days. The dried organs were weighed, and the roots and shoots of each plant were combined and ground into a fine powder. The samples were analyzed using an isotope ratio mass spectrometer (Isorime100; Elementar Analysensysteme, Hanau, Germany). The rate of  $^{15}\text{NO}_3^-$  or  $^{15}\text{NH}_4^+$  uptake was calculated from the total  $^{15}\text{N}$  of the plant and the biomass of the roots.

To measure the total N content, the shoots of the plants were dried at 65°C for 3 days and digested using sulfuric

acid at 360°C–380°C until the mixture cleared. Then, a few drops of  $\text{H}_2\text{O}_2$  solution (30%) were added to the mixture and further digested until the brown mixture turned colorless. The total N content in the digest was determined using the phenol-hypochlorite method ([Vega-Mas et al., 2015](#)). N uptake efficiency was calculated as shoot N to N in pots, and NUE as dry shoot biomass to N in pots ([Perchlik and Tegeder, 2018](#); [Weih et al., 2018](#)).

### Analysis of pH and visualization of rhizosphere alkalization

The pH indicator bromocresol purple (0.006%; Sigma-Aldrich) was used to visualize rhizosphere acidification. Roots were embedded in a complete nutrient medium solidified by the addition of 0.6% (w/v) type II agarose (Sigma). The initial pH of the agarose medium was adjusted to 4.8. Images were acquired at 16 h.

The time course of pH alterations in the rooting medium with an initial pH of 4.8 was measured in a hydroponic-based system. Plants were cultured in a hydroponic system for 3 weeks, as described in [Fang et al. \(2016\)](#), before being transferred to an acidic growth medium. Two seedlings were grown per pot. The pH of the rooting medium was measured using a pH electrode at the indicated times.

### Analysis of green fluorescent protein and histochemical staining

After 1 day of low-pH treatment, GFP-STOP1 expression in the roots of *pSTOP1:GFP-STOP1* transgenic plants was detected using a confocal laser-scanning microscope (LSM880; Zeiss). The excitation and emission wavelengths were 488 nm/500–530 nm for GFP protein. Images were analyzed using the ZEN 2012 Blue Edition and ImageJ2X software.

For GUS activity analysis, the roots of plants after 1 day of low-pH treatment were used for histochemical staining. The histochemical staining of GUS in the roots of *pNRT1.1:GUS* and *pNRT1.1:GUS/stop1<sup>KO</sup>* plants was performed as described in [Béziat et al. \(2017\)](#). The spatial quantification of GUS activity in the roots of *pNRT1.1:GUS* plants was performed using the freely available image analysis software ImageJ2X ([Béziat et al., 2017](#)).

The PM integrity of the root was evaluated by staining with 0.5% (w/v) of Evans blue using a microscope.

### Plasmid construction and transient expression assay

The full-length promoter region (4.5 kb) of *NRT1.1* was divided into three segments (P1, P2, and P3). The P1 segments were further divided into four segments, as shown in [Figure 6A](#). The fragments were individually inserted into the modified reporter vector *pGreen0800-LUC* using XhoI and BamHI restriction sites. The STOP1 effector construct was 35S:STOP1. The full-length *STOP1* protein-coding sequence was amplified by PCR and inserted into pCAMBIA1300 using Sall and KpnI restriction sites. The primers used to generate the various clones are listed in [Supplemental Data Set S1](#). In dual-luciferase reporter assays, reporter and effector



constructs were co-transformed into young *N. benthamiana* leaves for 48–72 h. Firefly and Renilla luciferase activities were quantified using a dual-luciferase assay kit (Beyotime Biotechnology, China) according to the manufacturer's instructions. The EV pCambia1300 was used as a negative control (set as 1). Some infiltrated leaves were also sprayed with 1 mM luciferin (A600577; Sangon Biotech, Shanghai, China) in the dark for 5 min before luminescence detection. The images of luminescence were captured using a cooled charge-coupled device imaging apparatus (LB985; Berthold). The images presented in the figures are representative of at least four *N. benthamiana* leaves.

### Quantitative reverse transcription polymerase chain reaction and CHIP-qPCR analysis

The expression of nitrate transporter (NRT) genes was determined using root samples. Total RNA was extracted from 50 to 100 mg of the tissue sample using RNAiso Plus (TaKaRa, Otsu, Japan), and 500 ng RNA was used to synthesize the first-strand cDNA using ReverTra Ace qPCR RT Master Mix with gDNA Remover (TOYOBO, Osaka, Japan). The expression of the corresponding genes was determined using the ChamQ Universal SYBR qPCR Master Mix (Q711-02; Vazyme Biotech Co., Ltd). The gene-specific primers used for quantitative PCR are listed in [Supplemental Data Set S1](#). Relative transcript levels were measured, and corrected efficiency calculations were conducted as previously described ([Fang et al., 2016](#)). Expression levels were normalized to the expression level of *UBIQUITIN 10*.

The agarose CHIP Kit (26156; Thermo Fisher Scientific) was used for CHIP assays. Seven-day-old *pSTOP1:GFP-STOP1* and Col-0 plants were treated with low pH for 1 day and then used for the isolation of chromatin. The sheared DNA was immunoprecipitated with an anti-GFP antibody (Cat. No. ab290, ChIP Grade; Abcam, USA) overnight at 50–100 rpm at 4°C. The enrichment of two *NRT1.1* promoter fragments in the immune precipitant was determined by qPCR using specific primers ([Supplemental Data Set S1](#)). The fold enrichment represents the immune-precipitation efficiency in the GFP-STOP1 transgenic plants normalized to that in the Col-0 plants.

### Purification of His-TF-tagged STOP1 and EMSA

The CDS of *STOP1* was PCR-amplified and cloned into the pCold-TF vector (TaKaRa, Japan), which enables fusion a hexahistidine-tagged trigger factor (His-TF) to enhance protein expression at low temperature. Isopropyl  $\beta$ -D-1 thiogalactopyranoside (1 mM) was supplied to *Escherichia coli* BL21 carrying pCold-TF-STOP1 at 16°C for 20 h to induce expression of the His-TF-STOP1 protein. Fresh cells were collected by centrifuging at 2,700g for 10 min. The cells were resuspended in lysis buffer (1 × phosphate buffered saline [PBS], 0.2 mg·mL<sup>-1</sup> lysozyme, 20  $\mu$ g·mL<sup>-1</sup> DNase, 1-mM MgCl<sub>2</sub>, and 1-mM phenylmethylsulfonyl fluoride [PMSF]) and sonicated. After centrifugation at 2,700g, 4°C for 10 min, the protein in the supernatant was collected using HisPur Ni-NTA Resin (Thermo Scientific) and was repeatedly

washed with wash buffer (1 × PBS, 1-mM PMSF, 10-mM imidazole, pH 8.0) until the absorbance at 280 nm reached baseline. Subsequently, elutions were performed with increments of imidazole step gradient but using an elution buffer containing 1 × PBS and 1-mM PMSF. Elution fractions were analyzed using sodium dodecyl sulfate–polyacrylamide gel electrophoresis. The fraction eluted with 300-mM imidazole was selected ([Supplemental Figure S20](#)). The selected fraction was further washed through a centrifugal filter (Merck Millipore, Amicon Ultra 15, molecular weight cut-off of 50,000 Da) to remove imidazole, and the concentrated protein was checked by immunoblot with anti-6 × His Tag mouse monoclonal antibody (Cat. No. 191001, Sangon Biotech, China; [Supplemental Figure S20](#)). To prepare the dsDNA probes and competitors, single-strand oligonucleotides were annealed by decreasing the temperature by 0.1°C every 8 s from 95°C to 4°C. Probes and competitors were amplified by PCR using biotin-labeled or nonlabeled primers ([Supplemental Data Set S1](#)). EMSA was carried out using a chemiluminescent EMSA kit according to the manufacturer's instructions (GS009; Beyotime Biotechnology, China).

### Statistical analyses

Data were analyzed by one-way or two-way analysis of variance (ANOVA) with Tukey's multiple comparison test. ANOVA results are listed in [Supplemental Data Set S2](#).

### Accession numbers

Sequence data from this article can be found in the Arabidopsis Genome Initiative or GenBank/EMBL databases under the following accession numbers: *STOP1* (AT1g34370), *NRT1.1* (AT1g12110), *NRT1.2* (AT1g69850), *NRT2.1* (AT1g08090), *NRT2.2* (AT1g08100), *NRT2.4* (AT5g60770), *NRT2.5* (AT1g12940), *AHA1* (AT2g18960), *AHA2* (AT4g30190), *AHA3* (AT5g57350), *AHA4* (AT3g47950), *AHA5* (AT2g24520), *AHA6* (AT2g07560), *AHA7* (AT3g60330), *AHA8* (AT3g42640), *AHA9* (AT1g80660), *AHA10* (AT1g17260), *AHA11* (AT5g62670), and *UBQ10* (AT4g05320).

### Supplemental data

The following materials are available in the online version of this article.

**Supplemental Figure S1.** Growth of *stop1* and *stop1*<sup>KO</sup> mutants in acidic and neutral soils.

**Supplemental Figure S2.** Col-0 and *stop1*<sup>KO</sup> co-planting improves the growth of *stop1*<sup>KO</sup> in acidic soil fertilized with nitrate.

**Supplemental Figure S3.** Root growth of mono-planted and co-planted seedlings in agar medium.

**Supplemental Figure S4.** Effect of Homo-PIPES on the root growth of Col-0 and *stop1*<sup>KO</sup> mutant in pH 6.5.

**Supplemental Figure S5.** Detection of the PM integrity of the root tissues by histochemical staining with Evans blue.

**Supplemental Figure S6.** RT-qPCR analyses of PM H<sup>+</sup>-ATPase genes in the roots of Col-0 and *stop1* mutants.

**Supplemental Figure S7.** Growth response of Col-0 and *stop1* mutants to low pH in the medium containing ammonium as a main N source.

**Supplemental Figure S8.** Effect of nitrate level on the rhizosphere pH of Col-0 and *stop1* mutants.

**Supplemental Figure S9.** Ammonium uptake of Col-0 and *stop1* mutants.

**Supplemental Figure S10.** RT-qPCR analyses of nitrate uptake-related genes in the roots of wild-type plants and *stop1* mutants.

**Supplemental Figure S11.** Effect of pH on STOP1 expression.

**Supplemental Figure S12.** Effect of nitrate level on STOP1 expression.

**Supplemental Figure S13.** Additional information of the transient dual-luciferase assays.

**Supplemental Figure S14.** Comparison of the STOP1-binding sites in the NRT1.1 promoter with some previously published motifs.

**Supplemental Figure S15.** Genotyping the *stop1 nrt1.1* double mutants by PCR.

**Supplemental Figure S16.** Effects of pH on the rate of nitrate uptake by roots of hydroponically grown plants.

**Supplemental Figure S17.** NRT1.1 expression and nitrate uptake rate in the root of Col-0, *stop1<sup>KO</sup>*, and *p35S:NRT1.1/stop1<sup>KO</sup>* transgenic plants at pH 4.8.

**Supplemental Figure S18.** Loss of CIPK23 function did not significantly affect the H<sup>+</sup> tolerance of plants.

**Supplemental Figure S19.** Nitrate uptake rate in the roots of *stop1* and *nrt1.1* mutants under different nitrate conditions.

**Supplemental Figure S20.** Sodium dodecyl sulfate–polyacrylamide gel electrophoresis and immunoblot analysis of purified His-TF-STOP1.

**Supplemental Table S1.** Physico-chemical properties of the soils used in studies.

**Supplemental Data Set S1.** Primers used in this study.

**Supplemental Data Set S2.** ANOVA statistics for this study.

## Acknowledgments

The authors thank Dr Thierry Desnos (Institut de Biosciences et Biotechnologie Aix-Marseille) for providing seeds. Dr Liang Ni (AES of Zhejiang University) is gratefully acknowledged for his assistance in seed propagation. We would like to thank Editage (www.editage.cn) for English language editing.

## Funding

This study was funded by the Zhejiang Province Natural Science Foundation (grant no. LZ21D010001).

*Conflict of interest statement.* The authors have no conflicts of interest to declare.

## References

- Aitken RL, Moody PW, McKinley PG (1990) Lime requirement of acidic Queensland soils. I. Relationship between soil properties and pH buffer capacity. *Aust J Soil Res* **28**: 695–701
- Baker CJ, Mock NM (1994) An improved method for monitoring cell death in cell suspension and leaf disc assays using Evans blue. *Plant Cell Tiss Organ Cult* **39**: 7–12
- Bagayoko M, Alvey S, Neumann G, Bürkert A (2000) Root-induced increases in soil pH and nutrient availability to field-grown cereals and legumes on acid sandy soils of Sudano-Sahelian West Africa. *Plant Soil* **225**: 117–127.
- Balzegue C, Dartevelle T, Godon C, Laugier E, Meisrimler C, Teulon JM, Creff A, Bissler M, Brouchoud C, Hagege A, et al. (2017) Low phosphate activates STOP1-ALMT1 to rapidly inhibit root cell elongation. *Nat Commun* **8**: 15300
- Bravin MN, Tentscher P, Rose J, Hinsinger P (2009) Rhizosphere pH gradient controls copper availability in a strongly acidic soil. *Environ Sci Technol* **43**: 5686–5691
- Béziat C, Kleine-Vehn J, Feraru E (2017) Plant hormones. In J Kleine-Vehn, M Sauer, eds, *Methods in Molecular Biology: Histochemical Staining of  $\beta$ -Glucuronidase and its Spatial Quantification*. Humana Press, New York, pp 73–80
- Chen K, Chen H, Tseng C, Tsay YF (2020) Improving nitrogen use efficiency by manipulating nitrate remobilization in plants. *Nat Plants* **6**: 1126–1135
- Enomoto T, Tokizawa M, Ito H, Iuchi S, Kobayashi M, Yamamoto YY, Kobayashi Y, Koyama H (2019) STOP1 regulates the expression of HsfA2 and GDHs that are critical for low-oxygen tolerance in Arabidopsis. *J Exp Bot* **70**: 3297–3311
- Falhof J, Pedersen JT, Fuglsang AT, Palmgren M (2016) Plasma membrane H<sup>+</sup>-ATPase regulation in the center of plant physiology. *Mol Plant* **9**: 323–337
- Fang XZ, Tian WH, Liu XX, Lin XY, Jin CW, Zheng SJ (2016) Alleviation of proton toxicity by nitrate uptake specifically depends on nitrate transporter 1.1 in Arabidopsis. *New Phytol* **211**: 149–158
- Fang Q, Zhang J, Zhang Y, Fan N, van den Burg HA, Huang CF (2020) Regulation of aluminum resistance in Arabidopsis involves the SUMOylation of the zinc finger transcription factor STOP1. *Plant Cell* **32**: 3921–3938
- Feng H, Fan X, Miller AJ, Xu G (2020) Plant nitrogen uptake and assimilation: regulation of cellular pH homeostasis. *J Exp Bot* **71**: 4380–4392
- Gijsman AJ (1990) Rhizosphere pH along different root zones of Douglas-fir (*Pseudotsuga menziesii*), as affected by source of nitrogen. *Plant Soil* **124**: 161–167
- Godon C, Mercier C, Wang XY, David P, Richaud P, Nussaume L, Liu D, Desnos T (2019) Under phosphate starvation conditions, Fe and Al trigger accumulation of the transcription factor STOP1 in the nucleus of Arabidopsis root cells. *Plant J* **99**: 937–949
- Guo JH, Liu XJ, Zhang Y, Shen JL, Han WX, Zhang WF, Christie P, Goulding KWT, Vitousek PM, Zhang FS (2010) Significant acidification in major Chinese croplands. *Science* **327**: 1008–1010
- Guo YX, Chen YF, Searchinger TD, Zhou M, Pan D, Yang JN, Wu L, Cui ZL, Zhang WF, Zhang FS, et al. (2020) Air quality, nitrogen use efficiency and food security in China are improved by cost-effective agricultural nitrogen management. *Nat Food* **1**: 648–658
- Haynes RJ (1990) Active ion uptake and maintenance of cation-anion balance: a critical examination of their role in regulating rhizosphere pH. *Plant Soil* **126**: 247–264
- Ho C, Lin S, Hu H, Tsay YF (2009) CHL1 functions as a nitrate sensor in plants. *Cell* **138**: 1184–1194
- Huang NC, Chiang CS, Crawford NM, Tsay YF (1996) CHL1 encodes a component of the low-affinity nitrate uptake system in Arabidopsis and shows cell type-specific expression in roots. *Plant Cell* **8**: 2183–2191
- Ito H, Kobayashi Y, Yamamoto YY, Koyama H (2019) Characterization of NtSTOP1-regulating genes in tobacco under aluminum stress. *Soil Sci Plant Nutr* **65**: 251–258

- Iuchi S, Koyama H, Iuchi A, Kobayashi Y, Kitabayashi S, Kobayashi Y, Ikka T, Hirayama T, Shinozaki K, Kobayashi M** (2007) Zinc finger protein STOP1 is critical for proton tolerance in Arabidopsis and coregulates a key gene in aluminum tolerance. *Proc Natl Acad Sci USA* **104**: 9900–9905
- Jadon P, Selladurai R, Yadav SS, Coumar MV, Dotaniya ML, Singh AK, Bhadouriya J, Kundu S** (2018) Volatilization and leaching losses of nitrogen from different coated urea fertilizers. *J Soil Sci Plant Nutr* **18**: 1036–1047
- Kissel DE, Bock BR, Ogles CZ** (2020) Thoughts on acidification of soils by nitrogen and sulfur fertilizers. *Agrosyst Geosci Environ* **3**: e20060
- Kobayashi Y, Kobayashi Y, Watanabe T, Shaff JE, Ohta H, Kochian LV, Wagatsuma T, Kinraide TB, Koyama H** (2013) Molecular and physiological analysis of  $Al^{3+}$  and  $H^+$  rhizotoxicities at moderately acidic conditions. *Plant Physiol* **163**: 180–192
- Kochian LV, Pineros MA, Liu J, Magalhaes JV** (2015) Plant adaptation to acid soils: the molecular basis for crop aluminum resistance. *Annu Rev Plant Biol* **66**: 571–598
- Lezhneva L, Kiba T, Feria-Bourrellier AB, Lafouge F, Boutet-Mercey S, Zoufan P, Sakakibara H, Daniel-Vedele F, Krapp A** (2014) The Arabidopsis nitrate transporter NRT2.5 plays a role in nitrate acquisition and remobilization in nitrogen-starved plants. *Plant J* **80**: 230–241
- Li Y, Chapman SJ, Nicol GW, Yao H** (2018) Nitrification and nitrifiers in acidic soils. *Soil Biol Biochem* **116**: 290–301
- Liu KH, Huang CY, Tsay YF** (1999) CHL1 is a dual-affinity nitrate transporter of Arabidopsis involved in multiple phases of nitrate uptake. *Plant Cell* **11**: 865–874
- Marschner H** (1995) *Mineral Nutrition of Higher Plants*, Ed 2. Academic Press, London.
- Mora-Macías J, Ojeda-Riveraa JO, Gutiérrez-Alanisa D, Yong-Villalobosa L, Oropéza-Aburto A, Raya-González J, Jiménez-Domínguez G, Chávez-Calvilloa G, Rellán-Álvarez R, Herrera-Estrella L** (2017) Malate-dependent Fe accumulation is a critical checkpoint in the root developmental response to low phosphate. *Proc Natl Acad Sci USA* **114**: 3563–3572
- Nelson PN, Su N** (2010) Soil pH buffering capacity: a descriptive function and its application to some acidic tropical soils. *Soil Res* **48**: 201–207
- O'Malley RC, Huang SSC, Song L, Lewsey MG, Bartlett A, Nery JR, Galli M, Gallavotti A, Ecker JR** (2016) Cistrome and epicistrome features shape the regulatory DNA landscape. *Cell* **165**: 1280–1292
- Pacifici E, Mambro RD, Iorio RD, Costantino P, Sabatini S** (2018) Acidic cell elongation drives cell differentiation in the *Arabidopsis* root. *EMBO J* **37**: 99134
- Pedersen JT, Falhof J, Ekberg K, Buch-Pedersen MJ, Palmgren M** (2015) Metal fluoride inhibition of a P-type  $H^+$  pump: stabilization of the phosphoenzyme intermediate contributes to post-translational pump activation. *J Biol Chem* **290**: 20396–20406
- Perchlik M, Tegeder M** (2018) Leaf amino acid supply affects photosynthetic and plant nitrogen use efficiency under nitrogen stress. *Plant Physiol* **178**: 174–188
- Sadhukhan A, Enomoto T, Kobayashi Y, Watanabe T, Iuchi S, Kobayashi M, Sahoo L, Yamamoto YY, Koyama H** (2019) Sensitive to proton rhizotoxicity1 regulates salt and drought tolerance of Arabidopsis thaliana through transcriptional regulation of CIPK23. *Plant Cell Physiol* **60**: 2113–2126
- Sawaki Y, Iuchi S, Kobayashi Y, Kobayashi Y, Ikka T, Sakurai N, Fujita M, Shinozaki K, Shibata D, Kobayashi M, et al.** (2009). STOP1 regulates multiple genes that protect Arabidopsis from proton and aluminum toxicities. *Plant Physiol* **150**: 281–294
- Schubert SSE, Mengel K** (1990) Effect of low pH of the root medium on proton release, growth, and nutrient uptake of field beans (*Vicia faba*). *Plant Soil* **124**: 239–244
- Schroeder JI, Delhaize E, Frommer WB, Guerinot ML, Harrison MJ, Herrera-Estrella L, Horie T, Kochains LV, Munns R, Nishizawa NK, et al.** (2013). Using membrane transporters to improve crops for sustainable food production. *Nature* **497**: 60–66
- Shavrukov Y, Hirai Y** (2015) Good and bad protons: genetic aspects of acidity stress responses in plants. *J Exp Bot* **67**: 15–30
- Shi RY, Ni N, Nkoh JN, Li JY, Xu RK, Qian W** (2019) Beneficial dual role of biochars in inhibiting soil acidification resulting from nitrification. *Chemosphere* **234**: 43–51
- Sigurdarson JJ, Svane S, Karring H** (2018) The molecular processes of urea hydrolysis in relation to ammonia emissions from agriculture. *Rev Environ Sci Biotechnol* **17**: 241–258
- Smiley RW** (1974) Rhizosphere pH as influenced by plants, soils and nitrogen fertilizers. *Soil Sci Soc Am J Abstr* **38**: 795–799
- Tian WH, Ye JY, Cui MQ, Chang JB, Liu Y, Li GX, Wu YR, Xu JM, Harberd NP, Mao CZ, et al.** (2021) A transcription factor STOP1-centered pathway coordinates ammonium and phosphate acquisition in *Arabidopsis*. *Mol. Plant* **14**: 1674–2052
- Tokizawa M, Kobayashi Y, Saito T, Kobayashi M, Iuchi S, Nomoto M, Tada Y, Yamamoto YY, Koyama H** (2015) SENSITIVE TO PROTON RHIZOTOXICITY1, CALMODULIN BINDING TRANSCRIPTION ACTIVATOR2, and other transcription factors are involved in ALUMINUM-ACTIVATED MALATE TRANSPORTER1 expression. *Plant Physiol* **167**: 991–1003
- Tokizawa M, Enomoto T, Ito H, Wu LJ, Kobayashi Y, Mora-Macias J, Armenta-Medina D, Iuchi S, Kobayashi M, Nomoto M, et al.** (2021) High affinity promoter binding of STOP1 is essential for early expression of novel aluminum-induced resistance genes GDH1 and GDH2 in Arabidopsis. *J Exp Bot* **72**: 2769–2789
- Tsay YF, Schroeder JI, Feldmann KA, Crawford NM** (1993) The herbicide sensitivity gene CM.1 of Arabidopsis encodes a nitrate-inducible nitrate transporter. *Cell* **72**: 705–713
- Vega-Mas I, Sarasketa A, Marino D** (2015) High-throughput quantification of ammonium content in Arabidopsis. *Bio-protocol* **16**
- Vidal EA, Alvarez JM, Araus V, Riveras E, Brooks MD, Krouk G, Ruffel S, Lejay L, Crawford NM, Coruzzi GM, et al.** (2020). Nitrate in 2020: thirty years from transport to signaling networks. *Plant Cell* **32**: 2094–2119
- Wang YY, Hsu P, Tsay Y** (2012) Uptake, allocation and signaling of nitrate. *Trends Plant Sci* **17**: 458–467
- Wang Y, Cheng Y, Chen K, Tsay YF** (2018) Nitrate transport, signaling, and use efficiency. *Annu Rev Plant Biol* **69**: 85–122
- Wang X, Wang HF, Chen Y, Sun MM, Wang Y, Chen YF** (2020) The transcription factor NIGT1.2 modulates both phosphate uptake and nitrate influx during phosphate starvation in Arabidopsis and maize. *Plant Cell* **32**: 3519–3534
- Weih M, Hamnér K, Pourazari F** (2018) Analyzing plant nutrient uptake and utilization efficiencies: comparison between crops and approaches. *Plant Soil* **430**: 7–21
- Xu J, Li HD, Chen LQ, Wang Y, Liu LL, He L, Wu WH** (2006) A protein kinase, interacting with two calcineurin B-like proteins, regulates  $K^+$  transporter AKT1 in Arabidopsis. *Cell* **125**: 1347–1360
- Xu G, Fan X, Miller AJ** (2012) Plant nitrogen assimilation and use efficiency. *Annu Rev Plant Biol* **63**: 153–182
- Zhang WF, Dou ZX, Hea P, Jua XT, Powlsonc D, Chadwickd D, Norsee D, Luf YL, Zhanga Y, Wua L, et al.** (2013) New technologies reduce greenhouse gas emissions from nitrogenous fertilizer in China. *Proc Natl Acad Sci USA* **110**: 8375–8380
- Zhang Y, Zhang J, Guo JL, Zhou FL, Singh S, Xu X, Xie Q, Yang ZB, Huang CF** (2019) F-box protein RAE1 regulates the stability of the aluminum-resistance transcription factor STOP1 in Arabidopsis. *Proc Natl Acad Sci USA* **116**: 319–327
- Zhu J, Fang XZ, Dai YJ, Zhu YX, Chen HS, Lin XY, Jin CW** (2019) Nitrate transporter 1.1 alleviates Pb toxicity in Arabidopsis by preventing rhizosphere acidification. *J Exp Bot* **70**: 6363–6374